Experimental Neurology 277 (2016) 124–138

Contents lists available at ScienceDirect

Experimental Neurology

journal homepage: www.elsevier.com/locate/yexnr

Disconnection and hyper-connectivity underlie reorganization after TBI: A rodent functional connectomic analysis

N.G. Harris [a,*], D.R. Verley [a], B.A. Gutman [b], P.M. Thompson [c], H.J. Yeh [d], J.A. Brown [e]

[a] UCLA Brain Research Center, Department of Neurosurgery, University of California, Los Angeles, USA
[b] Imaging Genetics Center, Institute for Neuroimaging and Informatics, Department of Neurology, Keck/USC School of Medicine, University of Southern California, Los Angeles, CA, USA
[c] Departments of Psychiatry, Engineering, Radiology, & Ophthalmology, Keck/USC School of Medicine, University of Southern California, Los Angeles, CA, USA
[d] Department of Neurology, University of California, Los Angeles, USA
[e] Department of Neurology, University of California at San Francisco School of Medicine, San Francisco, CA, USA

ARTICLE INFO

Article history:
Received 8 September 2015
Received in revised form 1 December 2015
Accepted 22 December 2015
Available online 28 December 2015

Keywords:
Plasticity
Reorganization
Bold
Resting state fMRI
Connectivity
Controlled cortical impact
Rat

ABSTRACT

While past neuroimaging methods have contributed greatly to our understanding of brain function after traumatic brain injury (TBI), resting state functional MRI (rsfMRI) connectivity methods have more recently provided a far more unbiased approach with which to monitor brain circuitry compared to task-based approaches. However, current knowledge on the physiologic underpinnings of the correlated blood oxygen level dependent signal, and how changes in functional connectivity relate to reorganizational processes that occur following injury is limited. The degree and extent of this relationship remain to be determined in order that rsfMRI methods can be fully adapted for determining the optimal timing and type of rehabilitative interventions that can be used post-TBI to achieve the best outcome. Very few rsfMRI studies exist after experimental TBI and therefore we chose to acquire rsfMRI data before and at 7, 14 and 28 days after experimental TBI using a well-known, clinically-relevant, unilateral controlled cortical impact injury (CCI) adult rat model of TBI. This model was chosen since it has widespread axonal injury, a well-defined time-course of reorganization including spine, dendrite, axonal and cortical map changes, as well as spontaneous recovery of sensorimotor function by 28 d post-injury from which to interpret alterations in functional connectivity. Data were co-registered to a parcellated rat template to generate adjacency matrices for network analysis by graph theory. Making no assumptions about direction of change, we used two-tailed statistical analysis over multiple brain regions in a data-driven approach to access global and regional changes in network topology in order to assess brain connectivity in an unbiased way. Our main hypothesis was that deficits in functional connectivity would become apparent in regions known to be structurally altered or deficient in axonal connectivity in this model. The data show the loss of functional connectivity predicted by the structural deficits, not only within the primary sensorimotor injury site and pericontused regions, but the normally connected homotopic cortex, as well as subcortical regions, all of which persisted chronically. Especially novel in this study is the unanticipated finding of widespread increases in connection strength that dwarf both the degree and extent of the functional disconnections, and which persist chronically in some sensorimotor and subcortically connected regions. Exploratory global network analysis showed changes in network parameters indicative of possible acutely increased random connectivity and temporary reductions in modularity that were matched by local increases in connectedness and increased efficiency among more weakly connected regions. The global network parameters: shortest path-length, clustering coefficient and modularity that were most affected by trauma also scaled with the severity of injury, so that the corresponding regional measures were correlated to the injury severity most notably at 7 and 14 days and especially within, but not limited to, the contralateral cortex. These changes in functional network parameters are discussed in relation to the known time-course of physiologic and anatomic data that underlie structural and functional reorganization in this experiment model of TBI.

1. Introduction

Traumatic brain injury (TBI) is often associated with diffuse white matter disconnections (Gennarelli et al., 1982; Graham et al., 1995) that can arise either due to a primary contusion injury or due to widespread axon shearing as a result of rapid head displacement. Both events

* Corresponding author at: UCLA Brain Injury Research Center, Department of Neurosurgery, David Geffen School of Medicine at UCLA, 300 Stein Plaza, Ste 535, Box 956901, Los Angeles, CA 90095-7039, USA.
E-mail address: ngharris@mednet.ucla.edu (N.G. Harris).

http://dx.doi.org/10.1016/j.expneurol.2015.12.020
0014-4886/

result in on-going loss of axonal integrity and disconnection. Altered functional connectivity that occurs as a consequence to and/or in addition to axonal disconnection is likely to be a major indicator of remaining brain function. As well as providing a potential marker for identifying regions of brain that may retain or gain function and/or structural plasticity, regions of altered functional connectivity may also be useful targets for rehabilitation therapy. However, compared to other CNS injuries such as stroke, there have been far fewer studies after TBI that have mapped remaining brain function in a longitudinal manner. As a result, there is a clear need for this type of research after TBI in order to establish how the brain responds to injury in order that we might tailor rehabilitative interventions to potentiate the spontaneous recovery that does occur.

Given that TBI often results in disparate regions of injury, resting state fMRI (rsfMRI) offers a significant advantage over task-based fMRI in that both the acquisition and analysis occur in a relatively unbiased way for identifying regional dysfunction. The technique enables multiple circuit abnormalities to be probed either as a data-driven or as an a-priori approach prior to dissecting more localized dysfunction with causal-based fMRI methods (David et al., 2008; Reyt et al., 2010; Rehme et al., 2011). Since the first rsfMRI publication showing the utility of resting state fMRI (Biswal et al., 1995), there has been a great deal of work that illustrates its sensitivity to altered brain function in a large number of disease states, indicating its potential as a clinical tool for diagnosing and monitoring dysfunction.

The potential for rsfMRI as a tool for following dynamic changes in functional organization has been demonstrated after stroke, both clinically (Wang et al., 2010) as well as in experimental models (van Meer et al., 2010; Magnuson et al., 2014a). Altered functional connectivity has also been shown after TBI, clinically (Nakamura et al., 2009; Kasahara et al., 2010, 2011; Mayer et al., 2011; Stevens et al., 2012; Pandit et al., 2013; Zhou et al., 2013; Han et al., 2014; Hillary et al., 2014) but with few studies in experimental models (Holschneider et al., 2013; Mishra et al., 2014) and no rsfMRI studies in the well-known controlled cortical impact (CCI) injury model of TBI where we have shown some degree of structural reorganization (Harris et al., 2009a) as well as functional reorganization (Harris et al., 2013a,b) that generally coincides with spontaneous recovery in this model.

Much is still unknown about the biology underlying the correlated blood-oxygen-level-dependent (BOLD) signal in terms of the structural correlate(s) that it underlies. In order to provide a more thorough understanding of how the known injury-related changes in brain structure and pathophysiologic processes relate to alterations in functional connectivity after TBI, a more detailed study of the temporal and spatial nature of injury-related changes in connectivity is required within a well-characterized experimental paradigm such as the CCI model (Chen et al., 2003). The longer-term goal is that by identifying the underlying processes driving the functional changes, we will then be in a position to begin to offer insights into the biologic substrate corresponding to changes in functional connectivity after TBI. As a result, we might then be able to address questions of how timing and intensity of rehabilitative interventions post-injury might be useful for shaping the degree and extent of functional network changes to improve outcome. Optimization of behavioral recovery by identification of CNS functional changes is still relatively understudied, and is an area that will benefit from identification of network architectural diagnostics that are predictive of outcome and/or altered brain function.

As a first step towards these goals, we acquired rsfMRI data before and at subsequent times after TBI using the rat CCI model and conducted network based analysis using graph theory. Making no assumptions about direction of change, we used two-tailed statistical analysis over multiple brain regions, and in a data-driven approach to access global and regional changes in network topology in order to assess brain connectivity in an unbiased way. Our main hypothesis was that deficits in functional connectivity would become apparent in regions known to be structurally altered or deficient in axonal connectivity in this model. Given the lack of functional network analysis data in models of TBI, a global analysis of multiple parameters was used as an initial, exploratory approach to provide an overview of connectivity at a range of network densities, before focusing at a regional level using more robust statistics. The results provide evidence post-injury reduction in connectivity as predicted by the known structural changes. However, we also found some compelling and somewhat surprising evidence of widespread hyper-connectivity that weaken as a function of time post-injury. These data are discussed with regard to the known alternations in brain structure and function in this model of TBI.

2. Methods

2.1. Experiment protocol

Resting state fMRI data were acquired on a 7 Tesla Bruker MRI from adult rats ($n = 15$) under medetomidine sedation before and at 7, 14 and 28 days after brain injury using the controlled cortical impact (CCI) model of TBI.

2.2. Brain injury

All study protocols were approved by the University of California Los Angeles Chancellor's Animal Research Committee and adhered to the Public Health Service Policy on Humane Care and Use of Laboratory Animals. The method for induction of moderate CCI injury was performed in the manner similar to previously described.(Chen et al., 2002, 2003, 2004; Harris et al., 2010a,b, 2012) Briefly, male, Sprague–Dawley rats (220–250 g body weight) were anesthetized with 2% isofluorane vaporized in O_2 flowing at 0.8 L/min and placed on a homeostatic temperature-controlled blanket while maintained in a stereotactic frame. CCI injury was produced using a 4 mm diameter impactor tip that was advanced through a 5 mm craniotomy (centered at 0.0 mm Bregma and 3 mm left-lateral to the sagittal suture) onto the brain using a 20 psi pressure pulse, and to a deformation depth of 2 mm below the dura. The craniotomy site was covered with a non-toxic, rapid curing silicone elastomer (WP Instruments, USA) and the wound was closed with sutures.

2.3. MRI acquisition

Rats were briefly anesthetized with 4% isofluorane in oxygen flowing at 0.6 l/min in order to administer medetomidine sedation (0.05 mg/kg in sterile saline, (Williams et al., 2010)) via the penile vein. Following placement of a subcutaneous cannula and initiation of continuous infusion of medetomidine (0.1 mg/kg/h), the rat was transferred to a purpose-built cradle and secured using three-point immobilization of the head with two ear bars and a tooth bar. Given the time-dependent effects of isoflurane on spontaneous bold fluctuations(Magnuson et al., 2014b), total exposure to isoflurane was minimized to 5–10 min after which the isoflurane was discontinued and the rat cradle was placed in the center of a 7 T magnet (Oxford Instr, Carteret, NJ, USA) spectrometer driven by a Bruker console running Paravision 5.1 (Billerica, MA USA). Respiration was monitored remotely and temperature was homoeothermically-controlled by forced air (SA11 Instr, Inc., USA). The S116 Bruker gradients (400 mT/m) were used in combination with a birdcage transmit and an actively decoupled receive-only surface coil to acquire the data. Following a multi-slice, gradient echo pilot scan to optimize positioning within the magnet, localized shimming was performed on the head to improve B0 homogeneity. A standard, single shot, gradient echo, echo planar imaging sequence was used to acquire 600 volumes (20 min) of resting state fMRI data. Images were acquired with a 128-read by 64-phase-encoding matrix (X,Y direction respectively) within a 30 mm^2 field-of-view and 14×0.75 mm contiguous, coronal slices, using a repetition/echo time TR/TE) of 2000/35 ms and 10 dummy scans prior to the acquisition. Anatomical, T2-weighted, Rapid-Relaxation-with-Enhancement (RARE) data

were then acquired using the same image resolution, at the same anatomical coordinates and using similar acquisition parameters except the following: matrix size — 128 × 128, TR/TE = 5000/ 60 ms, RARE factor 8, and 2 averages. Animals were recovered after imaging by reversing the sedation with Atipamezol (1 mg/kg, i.p.)

2.4. Data analysis

rsfMRI Data were weighted Fourier transformed to 128 × 128 and converted to compressed NIFTI format after which they were pre-processed (Fig. 1) for motion correction to generate nuisance parameters and then brain extracted (Smith, 2002). Contusion injury results in the formation of a CSF-filled cavity over the first few days post-injury in this model and inclusion of data from this region was prevented in two ways: (1) cerebrospinal fluid (CSF) signal was sampled in 2–4 voxels/slice within 2 slices per brain using ROI's delineated on the anatomical T2 data. The voxel-averaged signal was determined over the entire rsfMRI time-course and regressed out of the data together with the motion correction nuisance parameters using FEAT, part of the FSL toolbox (Smith et al., 2004) and in accordance with optimal methods for delineating regional signal correlations in the rat (Kalthoff et al., 2011). (2) Adjacency matrix data with zero correlations were removed from each rat brain prior to subsequent analysis to prevent any bias to non-intact brain tissue. Although this invariably results in the representation of contusion core data from the most mildly-injured rats, this did prevent non-intact brain regions from being assessed. The data were then slice-time corrected, Gaussian smoothed to 0.5 mm FWHM and then band-passed filtered at 0.01–0.25 Hz. This bandwidth was chosen since it includes the higher frequency blood-oxygen-level-dependent signal components present when under medetomidine sedation (Pan et al., 2013). Finally, data were warped to an anatomical template of the adult rat brain using an implementation of FSL FLIRT(Jenkinson and Smith, 2001; Jenkinson et al., 2002) adapted for the rat (Crum et al., 2013). The atlas was constructed by co-registering a parcellated cortical atlas (Valdés-Hernández et al., 2011) with subcortical structures (https://www.nitrc.org/projects/dti_rat_atlas/) together with numerous other structures from our in-house atlas which itself was manually constructed in 3-dimensions using Itksnap (Yushkevich et al., 2006) with reference to a 2-dimensional atlas (Paxinos and Watson, 1997). The final atlas consisted of 148 individual, parcellated regions.

We elected not to analyze regions posterior to Bregma −4.16 mm because the signal distortion around the ear canals that occurs when using a gradient echo, echo planar sequence prevents accurate warping of the posterior brain to a template. As a result, functional adjacency matrices were calculated from the time-series rsfMRI data using just 96 brain regions to obtain correlation coefficients that were then z-transformed. Given the controversy over anti-correlated networks and the fact that their existence varies with anesthetic state (Liang et al., 2012), we elected to investigate only positive correlations. We used graph theory parameters which were computed using the Brain Connectivity Tool Box (Rubinov and Sporns, 2010) and statistical analysis implemented in Matlab Statistical Toolbox (The Mathworks, Natick. MA) with display using Brainnet viewer (Xia et al., 2013) and Brainsuite software (Shattuck and Leahy, 2002).

We used the undirected, weighted, functional connectivity matrices to investigate theoretical measures of global and regional connectivity. The choice of weighted over binary network analysis was made based on the assumption that injury results in both increases and decreases in a whole host of anatomical and functional changes. Such changes could include axonal and dendrite sprouting, changes in synaptic number and function, alterations in receptor binding potentials, and cell

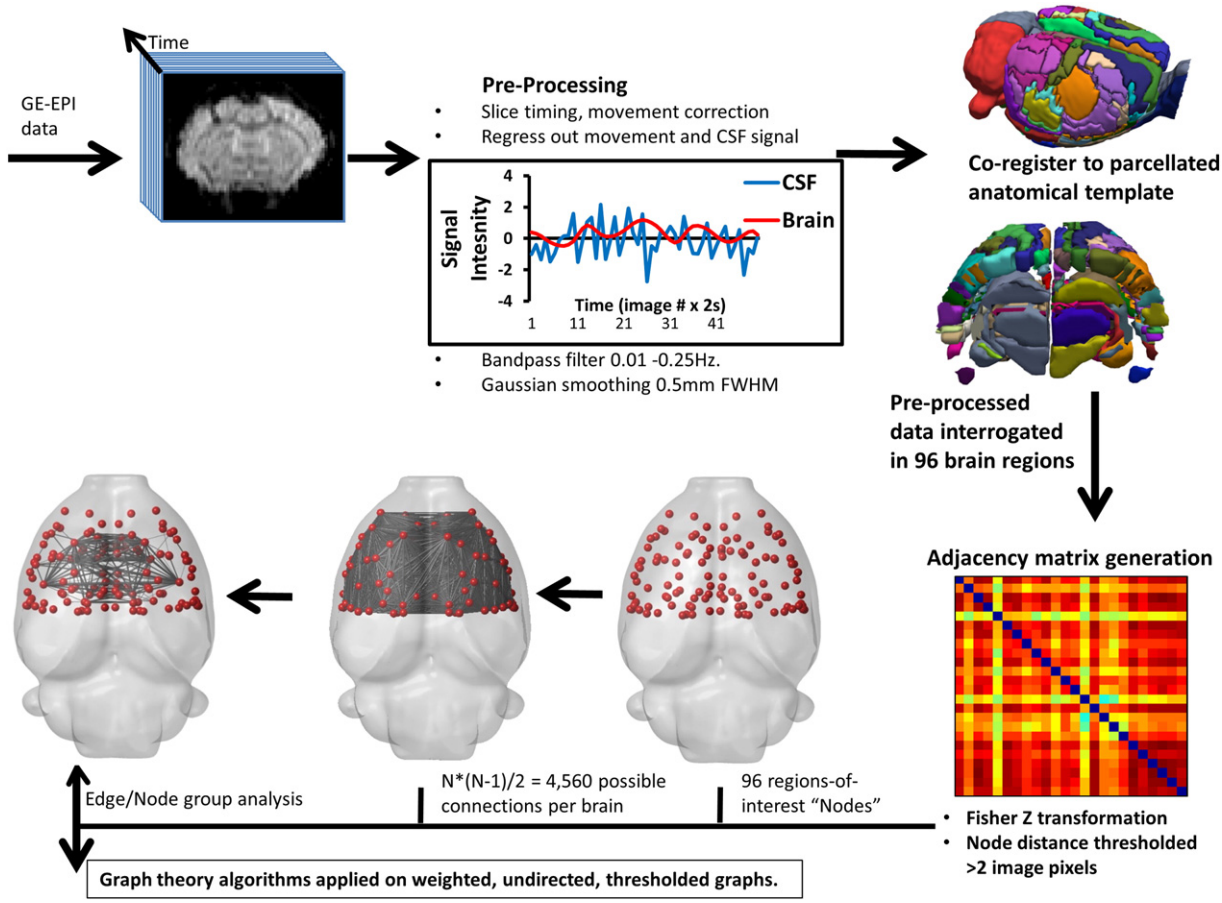

Fig. 1. Network analysis pipeline used for rodent brain.

excitability, to name a few. As a result, regional functional disconnection would unlikely be an all-or-nothing, binary phenomena modeled at a particular connection threshold, rather it is likely a result of a change in degree of connectedness or connection strength that can only be modeled through a weighted network analysis. We measured: (1) connection strength — the sum of the weighted edges connected to each node. (2) Characteristic shortest path length (CPL) — the average shortest number of weighted edges connecting between any two nodes in the brain. (3) Global efficiency (EGLOB) — the grand mean of the inverse distance across all nodes in the brain, which provides an indication of global integration of information across the brain globally in parallel. (4) Mean and regional local efficiency (MELOC and EREG respectively) — the regional local subnet mean and grand local mean, respectively of the inverse distance across all nodes in the brain or local subnet which provides an indication of local integration of information across the brain locally. (5) Mean clustering coefficient (MCC) — the ratio of connected neighboring nodes among all first-degree neighbors of a given node — an indication of the local connectivity for integration of information. (6) Modularity (Q) — the degree to which a network is organized into distinct communities of nodes with high intramodular and low intermodular connectivity, was determined by averaging over 100 iterations of the algorithm to account for random differences in module assignments from between run. (7) Betweeness centrality — the fraction of shortest paths that traverse an edge or node, and indication of the relative importance of a pathway. (8) Normalized CPL (lambda) and (9) normalized CC (gamma) were computed from the average comparison of each rat brain network with one hundred random networks containing a similar number of nodes, edges and network connectivity. (10) Small worldness — the ratio of gamma to lambda where a value greater than 1 indicates the network property of high local connectedness while maintaining a relatively low CPL. Contusion volume at 28 days post-injury was estimated from the T2-weighted, anatomical data by summing the volume of the ipsilateral cortical voxels with a greyscale intensity greater than 2 standard deviations above the mean intensity of the cortical gray matter of the hemisphere opposite the primary injury site.

2.5. Statistics

For the global parameter analysis we used a 2-tailed t test for determination of group difference at $P < 0.05$. Given that we a had no a priori information to inform on which network density would be useful in assessing any injury-related change, we elected not to perform statistical corrections for multi-level network density analysis. The intent was to use this as an initial, exploratory approach from which to focus on differences in connectivity at a regional level using more robust statistics. Group differences in regional node and edge analyses were tested for using 2-tailed t tests at $P < 0.05$ but corrected for multiple nodal comparisons using the false discovery rate at $q = 0.05$ and 0.005, for node and edge data respectively based on the number of potential comparisons.

3. Results

3.1. Alterations in global measures of connectivity

We first considered the group averaged connectomes as an initial gross readout of functional connectivity changes in the brain after injury. The pre-injury group mean adjacency matrix plot revealed BOLD signal regions that were highly correlated bilaterally within the brain, interspersed with more weakly correlated regions (Fig. 2A). Matrix subtraction plots of the post-injured brain compared to pre-injury revealed increases in regional correlation coefficients that occurred within 7 days in all brain regions apart from the primary injury site (Fig. 2B). This global increase in brain functional connectivity persisted at 14 days (Fig. 2C) and remained higher than pre-injury at 28 days when assessed globally over all regions as total weights of functional connectivity (Fig. 2E). However, despite these increases in functional connectivity, pericontusional connectivity and the corresponding homotopic regions exhibited much lower correlations compared to pre-injury at 28 days, indicating subsequent focal functional disconnection (Fig. 2D).

As an initial exploratory measure, global parameters of connectivity were assessed at a range of network density levels to determine reproducibility of the network measures within the current data. We chose to look at 0–50% density ranges given that higher density levels are likely to include increasing random connectivity that is unlikely to be biologically plausible. Since differences in nodal connectedness may complicate or even invalidate comparisons between groups when using a single, global threshold level, we determined the average network density level at which all graphs become fully connected to determine group difference. We found that graphs from rats before injury and at 14 and 28 d post-injury showed very similar numbers of components for each network density level, and graphs were fully connected respectively at $72 \pm 5.1\%$, 72 ± 3.6 and $72 \pm 4.0\%$ density (pre-injury, 14d and 28 d post-injury, respectively, $P > 0.05$, uncorrected, compared to pre-injury). At 7 d post-injury, the threshold for full graph connectivity was slightly higher ($80 \pm 4.6\%$), although this was not significant from pre-injury. These data therefore indicate that the comparison between groups at the same density levels is valid for this analysis.

3.2. Persistent decreases in shortest path and temporary decreases in small worldness indicate more random connectivity post-injury

Of all the global parameters assessed, characteristic shortest path length (CPL), the average of the number of edges traversed along the shortest path between any two nodes on the network, was particularly sensitive to injury because there were significant post-injury reductions regardless of density level at 7 and 14 days, and from all but the very strongest (most highly correlated) connections at 28 days ($P < 0.05$, uncorrected, Fig. 3A). Despite this robust finding however, changes in the global and mean local efficiency of the network (EGLOB, MELOC), the inverse of the average global CPL and local/nodal CPL respectively, were relatively less marked after injury, with no changes at the sparse network density levels containing the strongest connections (Fig. 3B,C). However, there were significant increases in both parameters at the weaker connection levels at all times after injury and this was especially the case within MELOC data ($P < 0.05$, Fig. 3B,C) implying a shift towards more efficient local connectivity and possibly some degree of network resilience to injury. Small worldness (SW), the network property reflecting a balance between segregation and integration of brain circuits, was also relatively unaffected by injury, although it consistently trended towards lower values at 7 days at all connection levels and was significant at the network density range 29–35% ($P < 0.05$, uncorrected, Fig. 3F), implying a shift in network topology towards a more randomly connected network. This temporary loss in SW ($SW < 1$) was driven mainly by alterations in normalized clustering coefficient (gamma), when compared to similarly connected random networks. This was reduced compared to pre-injury at all density levels towards values approaching 1, indicative of more random connectivity ($P < 0.05$, uncorrected, density range 25–36%, Fig. 3E). Normalized CPL (lambda) was a less likely driver of the loss of SW at 7 days post-injury because it was not significantly different over the same density range, although it trended lower than pre-injury at all levels at this time post-injury and was significantly lower among the stronger connections ($P < 0.05$, uncorrected, density range 4–19%, Fig. 3D), implying a shift towards shorter, more random paths especially within highly connected hub regions.

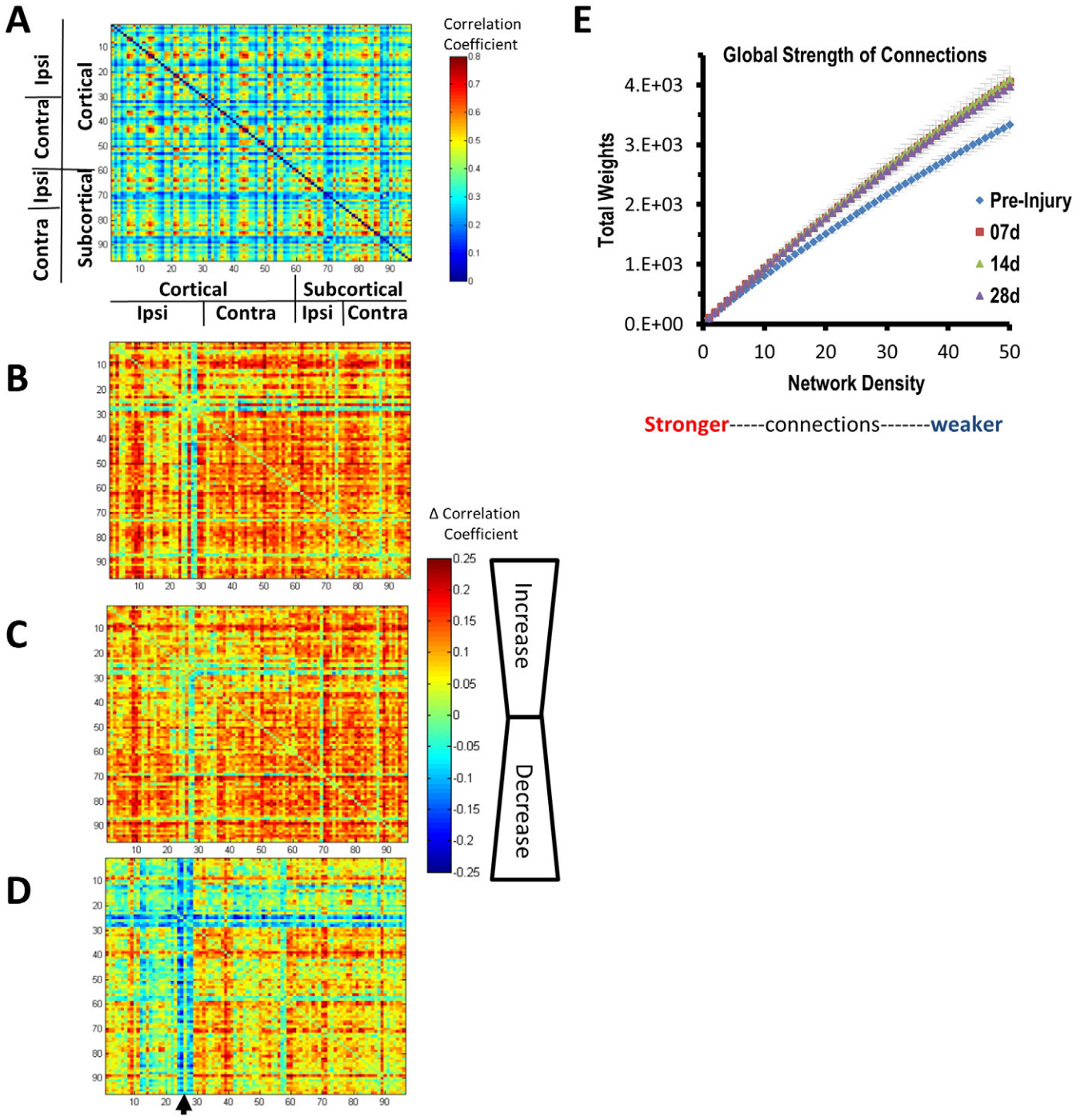

Fig. 2. Gross changes in functional correlation post-injury. [A] The pre-injury, group mean correlation matrix for all 96 regions examined and group mean difference matrices (injured − pre-injury) for [B] 7 days, [C] 14 days and [D] 28 days after injury showing that in addition to the expected decreases in ipsilateral S1 connectivity at 28 days (arrow in [D]) there were widespread increases in regional BOLD signal correlation coefficients at 7 and 14 days which persisted in contralateral cortical and bilateral subcortical areas to 28 days post-injury. [E] The total weight of connections over the whole brain was significantly greater at all times after injury and at all network density levels examined ($P < 0.05$, 2-tailed t-test). The greatest difference to pre-injury was clearly among the more weakly connected regions at the higher range of density values. All matrices were unthresholded at the 35% density level.

3.3. Regional measures of connectivity: predicted loss in functional connectivity, but unexpected increase in strength that persists chronically

Given the relatively robust global changes in functional connectivity and associated measures of network architecture after injury (Figs. 2, 3), we were particularly interested in looking at regional alterations to determine whether damage at the level of the primary injury site was driving the global changes, or whether there were more widespread disruptions. In the absence of any robust rationale for a threshold of connection strength being used to determine the presence or absence of edge connectivity, we show regional data calculated at 35% network density in order to provide data more representative of the global changes that were obtained at a range of density values. Additional data obtained at 10% density showed changes similar to those herein, but are not shown for clarity.

We first looked at the nodal strength, the sum of the weights of the links connected to each node (correlation coefficients) and found that as predicted by the well-known loss in structural connectivity of the

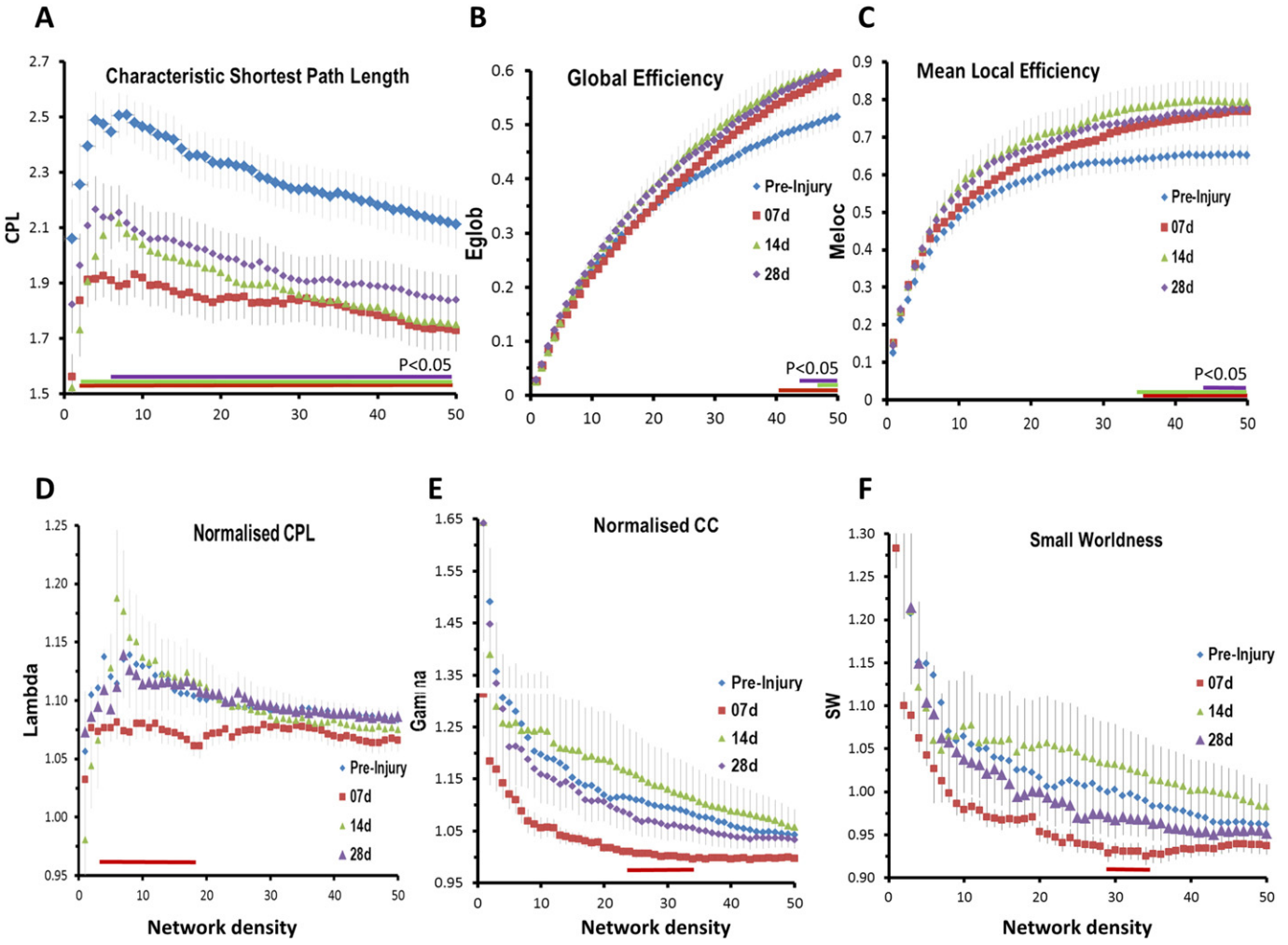

Fig. 3. Global measures of network connectivity after TBI. [A] The characteristic shortest path length (CPL) was significantly reduced from pre-injury values at all times after injury and at all connection strengths. This was particularly evident at 7 days after injury and although CPL values partially resolved towards pre-injury levels among the strongest connections at 14 days, and among all density levels by 28 days, CPL remained significantly shorter than pre-injury at the majority of density levels examined. [B] Global efficiency (Eglob) and [C] mean local efficiency (Meloc) were significantly increased at all times after injury but only among the weaker connections levels. Normalized CPL and CC were reduced from pre-injury only at 7 days after injury and only significantly at small density ranges. The quotient of these at 7 days small worldness was also lower overall density ranges compared to pre-injury. Data are means ± sems; colored horizontal bars indicate $P < 0.05$ compared to pre-injury, two-tailed t-test).

traumatically injured brain, there was a loss of nodal strength within the pericontusion site when compared to pre-injury values beginning at 7 days post-injury among ipsi-lesional sensory cortex (S1) trunk region, lateral parietal cortex, fornix (FDR $q = 0.05$) and S1 hind-limb region ($P < 0.05$, uncorrected, Fig. 4A,B). However, this only constituted 4% of the total number of nodes, and this rebounded at 14 days when there were no significant reductions compared to pre-injury. This latter effect is possibly related to within group differences of injury severity, since connection strength was most robustly correlated to degree of injury at 14 days (see below). By 28 days the number of nodes with reduced strength had expanded to 7% of all nodes to include ipsi-lesional S1 trunk/forelimb/hindlimb/dysgranular cortical regions (FDR $q = 0.05$, two tailed t test, Fig. 4A,B) and ipsi-lesional motor cortex (M1) and S1 shoulder regions ($P < 0.05$, uncorrected). Reduction in edge strength connectivity values largely followed the corresponding nodal reductions, with significant loss of inter-hemispheric cortical functional connectivity at 7 days (10 and 28% of the total edge reductions occurred in S1 trunk and S1 hind-limb cortex, respectively, FDR $q = 0.005$). Edge functional connectivity changes were minor at 14 days but at 28 days there was a further loss compared to 7 days and an expansion of disconnected regions of reduced functional connectivity, including cortex (10–14% reduction in edge strength occurred within S1 hind-limb/trunk/forelimb cortex as well as numerous bilateral subcortical regions, FDR $q = 0.005$ two tailed, Fig. 4A,B, as summarized in Fig. 5A).

Unexpectedly for this injury model, but as prefaced by the global changes represented by the group matrix values (Fig. 2), we found significant post-injury increases in connection strength, both at the nodal as well as the edge level that dwarfed the earlier reported reduction in strength (Figs. 6A,B versus 4A, B and summarized in 5A versus 5B). Nodal connection strength was increased in 34% of all nodes considered, and 24% of all nodes passed FDR correction at 7 days post-injury compared to pre-injury (FDR $q = 0.05$, two-tailed, Fig. 6A,B) indicating a very robust increase. Although the greatest increases in node strength at 7 days were constrained mostly to bilateral sensory and motor regions of the cortex, there were very significant subcortical increases within the highly connected hub nodes: ipsi-lesional hippocampus, thalamus and hypothalamus, as well as bilaterally in the caudate putamen/globus palidus (FDR $q = 0.05$,two-tailed). Increases in node strength persisted at 14 days (31% of nodes increased, 21% passing FDR correction) and included contra-lesional subcortical regions of thalamus, hippocampus and fimbria (FDR, $q = 0.05$). While 38% of nodes were still greater than pre-injury values at 28 days, only 15% survived FDR correction. This gradual normalization of nodal connection strength post-injury was largely constrained bilaterally to the cortex and contra-

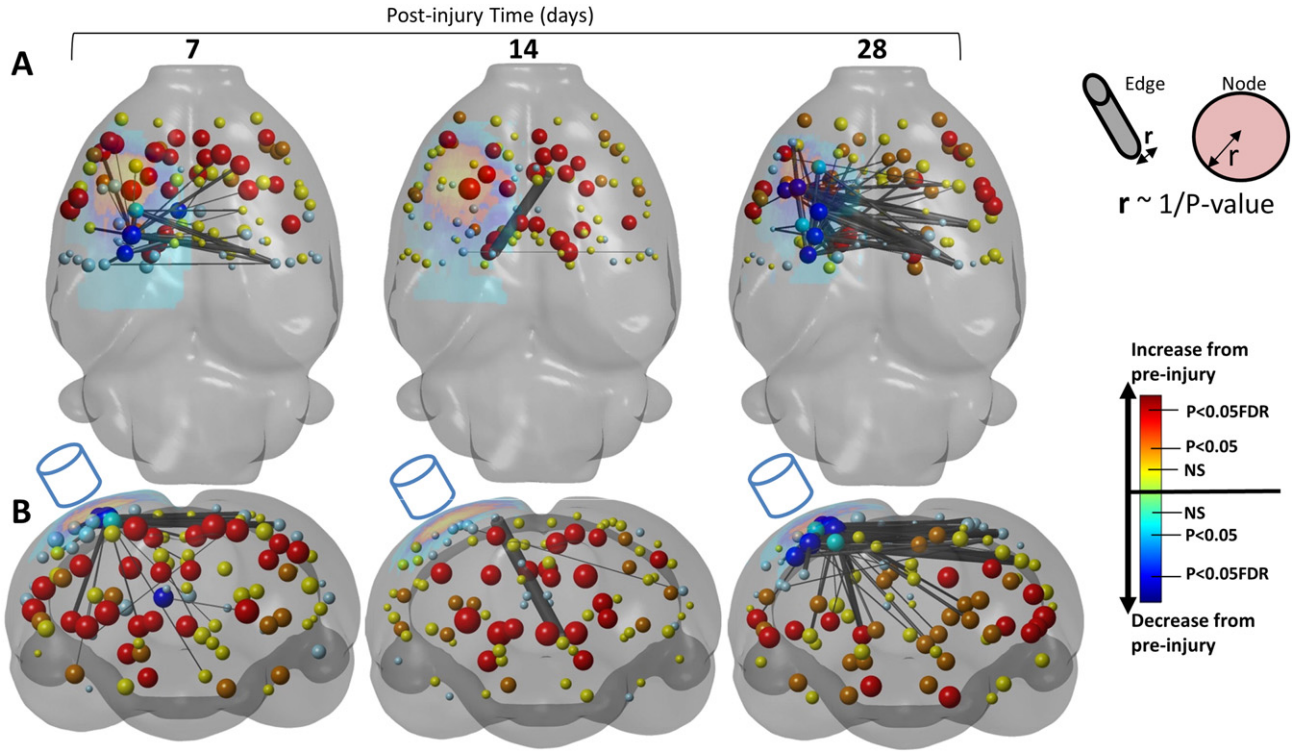

Fig. 4. Loss of functional connectivity. [A] Axial and [B] coronal, 3-dimensional-rendered statistical difference plots of node and decrease in edge strength at 7, 14 and 28 days after contusion injury (surface-projected yellow region on left of each brain ~ mean contusion volume) compared to pre-injured showing the brain regions of significant loss of functional connectivity (edge strength, black/gray bars, $P < 0.005$ FDR corrected) that occur mainly within regions of significant loss of nodal connectedness (node strength spheres, dark blue — $q = 0.05$, FDR-corrected, turquoise — $P < 0.05$, uncorrected, light blue — decrease from pre-injury $P > 0.05$). There was a loss of connectivity around peri-contusional regions (edges of yellow surface-projected region plotted on the left of each brain) at 7 days post-injury combined with some early loss of inter-hemispheric and subcortical connectivity. This was less evident at 14 days but became even more pronounced at 28 days. Key: node and edge radii are equivalent to the reciprocal of the P value between pre- and post-injury time-point of connection strength. Node colors represent the probability levels that describe the difference compared to pre-injury. Red — increase from pre-injury ($q = 0.05$, FDR-corrected) orange — increase from pre-injury ($P < 0.05$, uncorrected), yellow circles — increase from pre-injury ($P > 0.05$).

lesionally within subcortical regions. However, there were notable, remaining significant increases in nodal strength at 28 days post-injury: bilaterally within S2 cortex, in some S1 regions, as well as in ipsilesional thalamus and caudate, and bilaterally in the hippocampus (FDR $q = 0.05$). Increases in edge strength followed a similar temporal pattern to the nodal increases, with 326 significant increases in edge functional connectivity at 7 days, but only 158 by 28 days compared to pre-injury (FDR $q = 0.005$ two tailed, Fig. 6A,B) and summarized in Fig. 5B. The brain regions that accounted for the increases in edge functional connectivity at 7 days were bilaterally in the M1 and prefrontal cortex, caudate putamen/globus pallidus and septum (3–6%/region of all significantly increased edges) as well as ipsi-lesionally within S1 cortex, thalamus, hypothalamus and hippocampus (4–6%/region of all significant edges) and contra-lesionally within S1 barrel and cingulate-1 cortical regions (3–4%/region of all significant edges). Persistently increased edge functional connectivity at 28 days was accounted for mainly by bilateral increases in thalamus and S2 cortex (3–9%/region of all significant edges) as well as in contra-lesional hippocampus, caudate putamen and ventral pallidum/medial forebrain bundle (Fig. 5B).

3.4. Subcortical nodal hierarchy is relatively unperturbed by cortical injury

We investigated alterations in nodal functional connectivity hierarchy (nodes ranked by connection strength) in an attempt to improve our understanding of more subtle functional connectivity changes that injury produces. As expected, nodal rank is dominated in the naive (pre-injured) rat by the equally, highly-connected subcortical hubs of the thalamus and caudate putamen/globus pallidus, as well as the cortical hubs of the motor M1 and S1BF cortex (Fig. 7A). Unsurprisingly by 7 days after injury, the ipsi-lesional cortical hubs (left M1, S1BF, Cg1) begin to fall in rank and progress to drop further in rank or even out of the top 20% of most highly connected nodes by 28 days (Fig. 7B). At the same time and together with the subcortical hubs, the upper ranked hubs become dominated by contra-lesional (right) cortical hubs (M1, S1 barrel and cingulate-1 cortex). Interestingly, the ipsilesional motor M2 cortex, a pericontusional region that consistently survives this injury and associated with spontaneous axon sprouting at 7 days post-injury (Harris et al., 2010b), substantially increased in rank at 7 days compared to all other hubs within the top 20% of nodes. However, by 14 days it returned almost to its original rank and by 28 days it dropped out of the most highly connected hub- regions. Despite the earlier reported increase in connection strength, subcortical regions changed very little in rank before and after injury and remained among the most highly connected regions of the rat brain.

3.5. Sustained post-injury increase in local connectedness occurs despite a temporary loss of community architecture

We investigated whether alterations in the local connectedness of brain regions might account for or at least be consistent with the indicators of more random connectivity that we observed in the global measures of functional connectivity. This was indeed the case at higher density ranges when evaluating the mean clustering coefficient (CC), an indicator of the average local connectivity of adjacent connected nodes. Global, post-injury CC values were significantly increased from pre-injury beginning at 7 days, and this effect persisted to 28 d days over the network density range ~ 20–50% (Fig. 8A). There were similar effects at the nodal level (Fig. 8B) where, apart from reductions in the

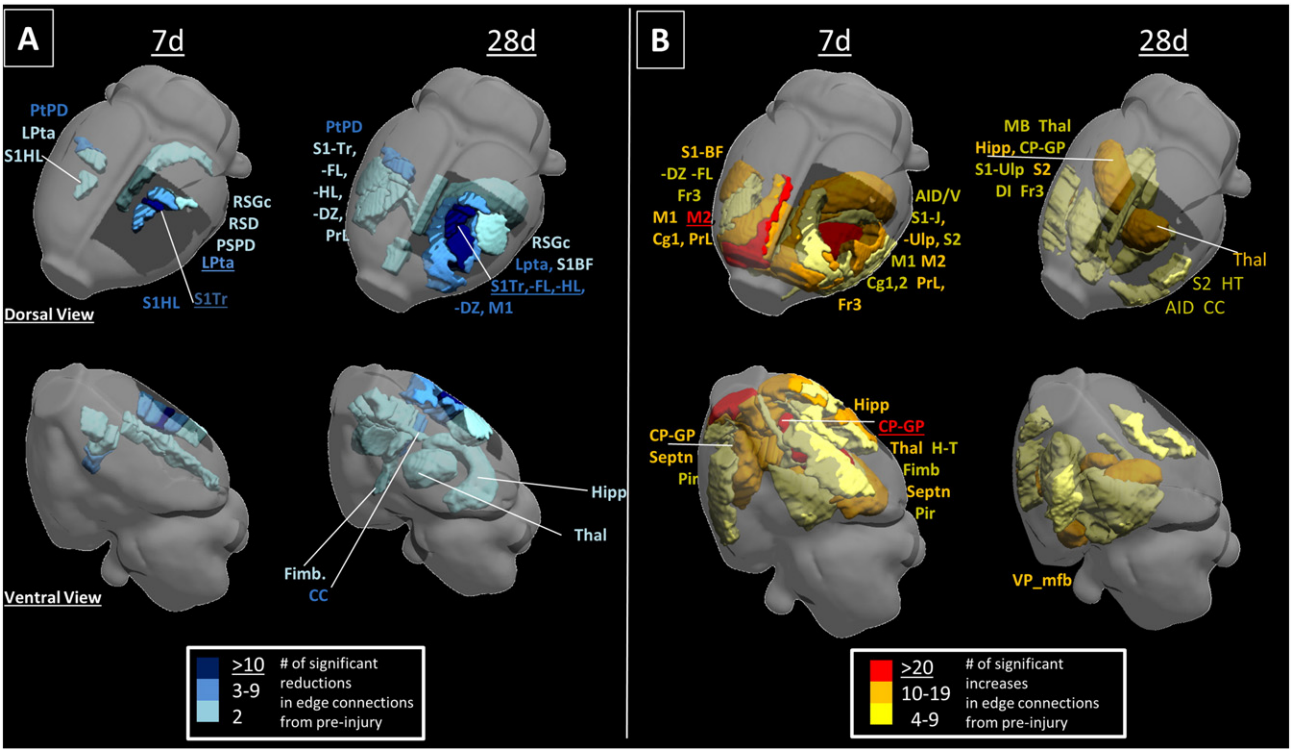

Fig. 5. Summary plots of edge connectivity changes after injury. The number of significant decreases [A] and increases [B] in edge connections per brain region at 7 and 28 days after injury compared to pre-injury was summed for all 96 nodes examined. The mean contusion volume is shown as a surface-projected black region. [A] Decreases in connectivity were relatively mild at 7 days after injury but this expanded to the ipsilateral cortex, thalamus and hippocampus and to the contralesional cortex by 28 days. [B] Increases in connectivity were especially marked early after injury in bilaterally in both cortical and subcortical regions. This persisted until 28 days only in bilateral subcortical regions and some contralesional and ipsilesional pericontusional regions. Key: colors denote the number of significant changes in connections compared to pre-injury.

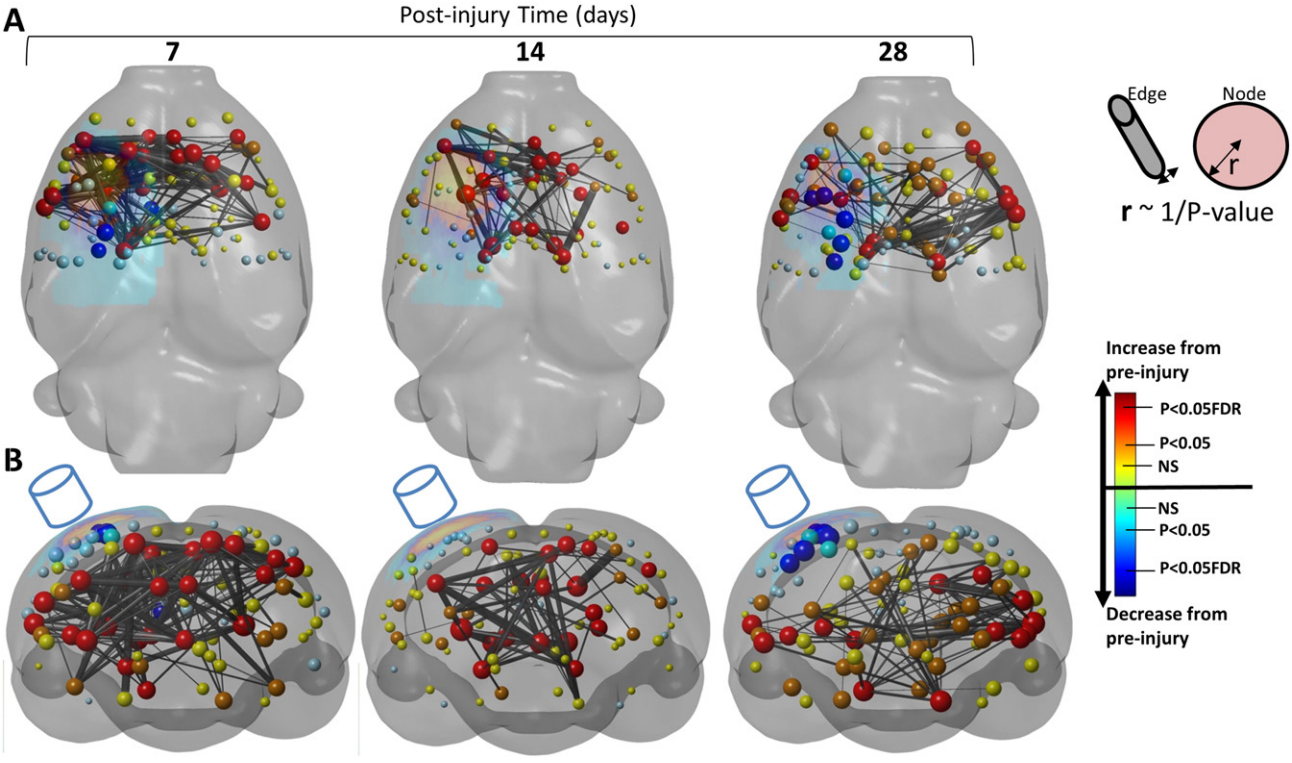

Fig. 6. Increase in functional connectivity. [A] Axial and [B] coronal, 3-dimensional-rendered statistical difference plots of node and increased in edge strength at 7, 14 and 28 days after injury compared to pre-injured showing the brain regions of significant increase in connectivity (edge strength, black/gray bars, q = 0.005 FDR corrected) that occur almost exclusively in regions of low nodal connectedness (node strength data is repeated here from Fig. 4). The greatest increase in connectivity occurred at 7 days after injury over wide areas of the brain. Increased connectivity persisted until 14 and 28 days where enhanced connections were largely subcortical and contra-lesional cortex. Key — see Fig. 3.

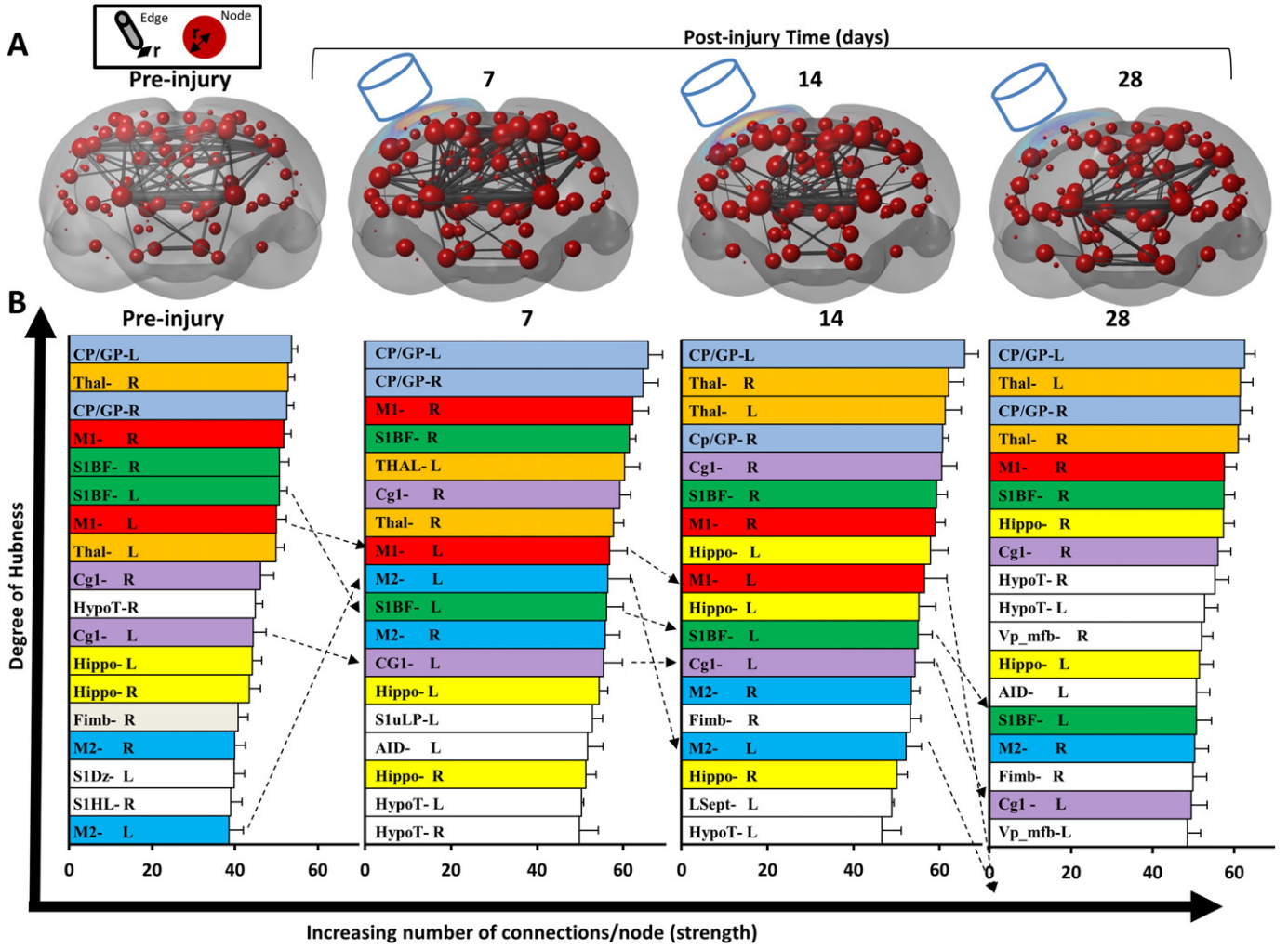

Fig. 7. Change in degree of hubness. [A] Coronal, 3-dimensional, rendered plots showing group mean node strength of connection (radii of node ~ mean number of weighted nodal connections at 35% network density) and mean connection strength between nodes among the top 2% of connections (edge radii ~ number of node-to-node connections) before and at 7, 14 and 28 days after injury. The average contusion size is superimposed on the left cortical surface and the cylinder represents the approximate impact of the injury device. [B] Mean node strength (the sum of the weights of the edges connected to each node at 35% network density) was calculated for each node, ranked at each time-point and the top 20% were plotted to assess the change among the most highly connected hub nodes. Injury resulted in progressive reductions in the rank of ipsi-lesional, highly connected cortical hubs that were adjacent to the primary injury site (S1BF-L, M1-L, Cg1-L) and also a transient increase in M2-L cortex at 7 days (hatched lines). Despite significant alterations in subcortical connectivity (see text), the Thal and CP-GP regions remained the most highly connected areas of the brain. Key: CP-GP = caudate putamen and globus pallidus, Cg1 = cingulate cortex, Fimb = fimbria, Hippo = hippocampus, HypoT = hypothalamus, M1, M2 = motor cortex, S1Dz/S1HL/S1uLP = sensory cortex dysgranular/hindlimb/upper lip region, L.Septn. = lateral septal nucleus, Thal = thalamus, Vp_mfb = ventral palladium and medial forebrain bundle.

primary injury site within S1Sh and adjacent cortex, there were widespread, significant increases in CC at 7 days (54% of all nodes, FDR, $q = 0.05$) that extended to 14 days (53% of all nodes, FDR, $q = 0.05$) and with less consistent increases at 28 days (44% of all nodes, $P < 0.05$, uncorrected only).

Based on the global network measures that indicate possibly temporary loss of SW and shorter, more random connectivity within the injured brain, as also reflected by the measured increases in local connectivity, it is conceivably that there is a period of hyperconnectivity during which the brain is redefining its local circuitry in order to circumvent the effects of injury. To determine whether this might be a plausible hypothesis, we investigated the functional segregation of the brain into network modules using the Louvain algorithm (Blondel et al., 2008) with the idea that in a more randomly connected brain, blurring of the boundaries between network modules that define the community-like architecture of the brain would be likely. The algorithm identifies communities of nodes based upon maximizing the number of intra-modular connections and minimizing the number of inter-modular connections within a subnet. A network with high modularity, Q, is one in which the ratio of intramodular edges to intermodular edges is high. Using 100 separate runs, the algorithm consistently divided up the rodent brain network into two main modules consisting of cortical and subcortical regions (Fig. 8C). The modularity Q levels showed very robust, significant decreases in modularity at 7 days post-injury when compared to pre-injury that were consistent over the full range of density levels examined (Fig. 8D), in agreement with our hypothesis. However, unlike the persistently increased CC values indicating increased local functional connectivity, this effect was only temporary because by 14 days modularity values were normalized and remained similar to pre-injury levels at 28 days.

3.6. Network-based differentiation between injury severities

Compared to other global parameters of connectivity, CPL, MCC and modularity were most profoundly affected by injury. Therefore we next looked at whether they would discriminate between different severities of injury, which occurred by chance in this cohort of rats, and which were well described by two different levels of contusion volume designated mild and moderate injury, based upon minimizing the within group variance of contusion volume. Mild and moderate injuries were

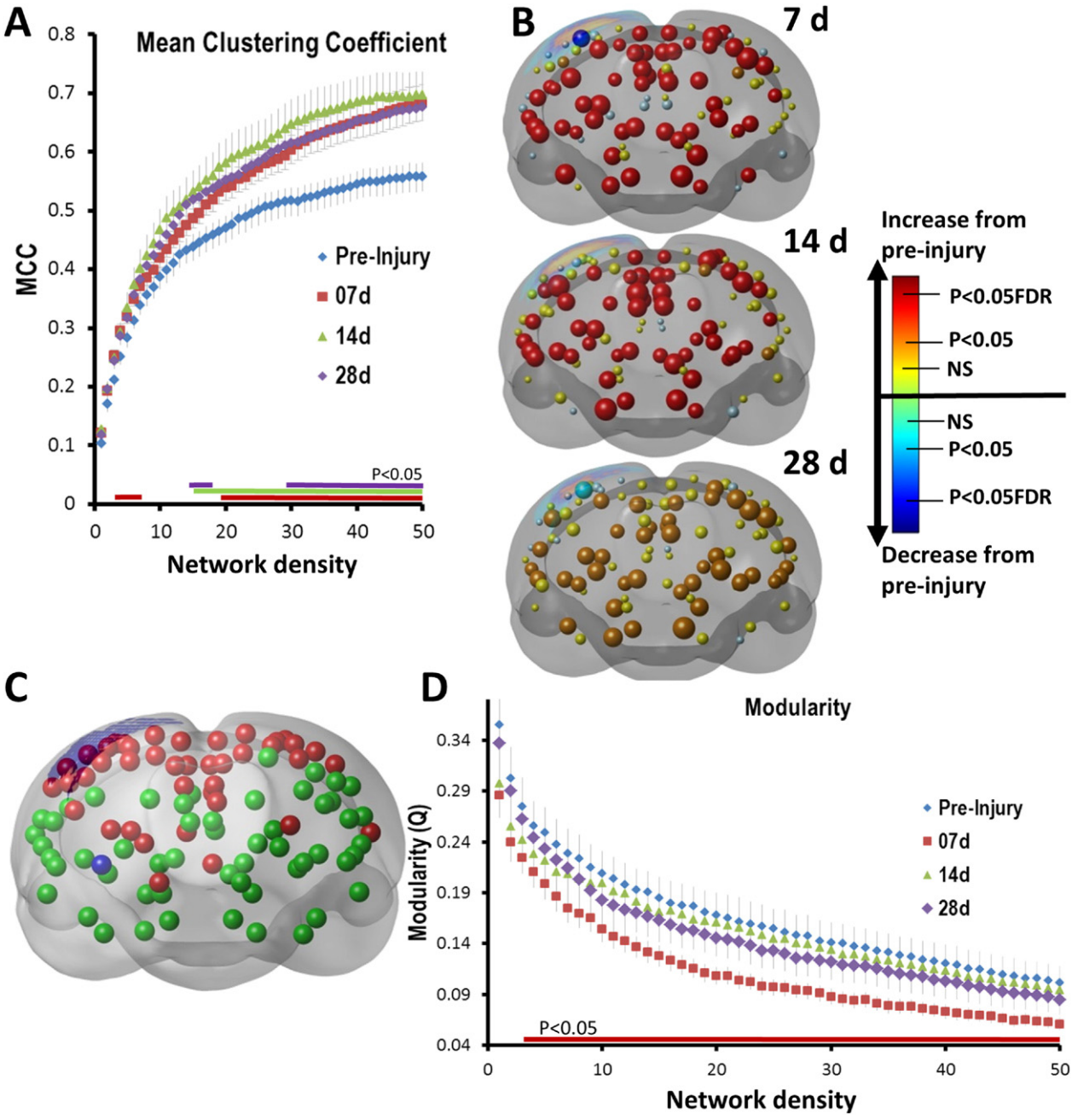

Fig. 8. Early and persistent increases in local connectedness and a temporary decrease in modularity. The mean clustering coefficient (MCC), an indication of the local connectedness of networks was assessed at [A] an average nodal (global) level and [B] a regional nodal level. [A] MCC was significantly increased from 7 days after injury compared to pre-injured over both strongly connected and at more weakly connected ranges (3–6%, 19–50%). This persisted until 28 d at 20–50% density levels (colored horizontal bars indicate $P < 0.05$ compared to pre-injury, two-tailed t-test; data are means ± sem). [B] 3-Dimensional, rendered, coronal plots of statistically different changes in regional (node) MCC at 7, 14 and 28 d post-injury compared to pre-injury. Apart from significant decreases in local connectedness within the primary cortical injury site (blue spheres; see Fig. 3 for key), there was a brain-wide increase in local connectivity that persisted among many regions for 14 days after injury (red spheres, $q = 0.05$, FDR corrected) and until 28 days (orange nodes, $P < 0.05$, uncorrected). [C] Modularity — the degree to which network circuitry is organized in a similar community structure was determined for unthresholded data over all groups. Two major modules were found corresponding to cortical and subcortical regions (red and green nodes, respectively). [D] Modularity was decreased at 7 days after injury, but not at any other time. This was significant over the majority of the density levels examined indicating a robust effect ($P < 0.05$, two-tailed t-test).

operationally defined within the current data based upon contusion volume at 28 days post-injury (mild = 2 ± 0.6 mm^3, n = 7; moderate = 20 ± 2 mm^3, n = 8, Fig. 9A,B). Modularity was assessed among the different injury severities at 7 days because it was significantly reduced from pre-injury only at that post-injury time within the pooled data (Fig. 8D). Although there were no overall significant differences in modularity due to injury severity ($P > 0.05$, 2-tailed t-test), there was a consistent trend towards lower global modularity after mild compared to moderate injury at almost all density levels (Fig. 9C). Within the context of their pre-injury values, this suggests that temporary loss of community structure was surprisingly greater in mild rather than moderate injury. CPL and MCC were similarly affected by injury severity at all times after injury and although differences between severity groups did not reach significance (with the exception of CPL at 14 days post-injury, Fig. 9E), moderate injury resulted in shorter CPL values and higher MCC values compared to mild injury at all density levels (Fig. 9D–I; $P > 0.05$, 2 tailed t test). Unlike modularity changes, mild injury CPL and MCC values remained closer to pre-injury values compared to moderate injury.

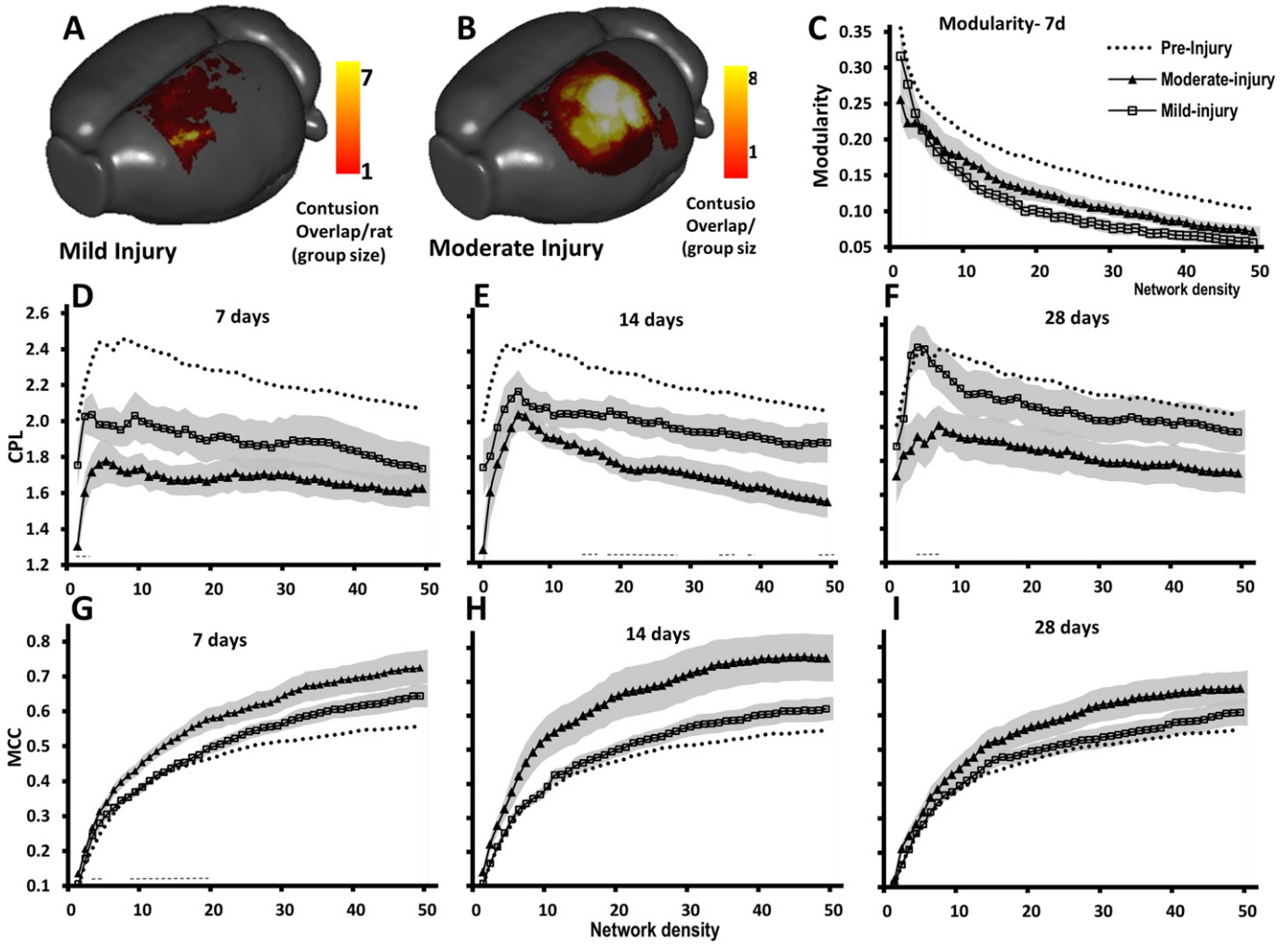

Fig. 9. Global CPL and MCC parameters of network-based functional connectivity do not significantly discriminate between different injury severities. Surface-projection plots of mean contusion size among [A] mild versus [B] moderately-injured rats at 28 days (color is equivalent to number of rats with an overlapping contusion site). Although there was a trend towards mild (square symbols) and moderate (triangular symbols) injury group differences in both global CPL [C–E] and MCC [F–H] network parameters at most density levels and at all time-after injury, CPL was significantly lower after moderate compared to mild injury, most notably at mid-range density values at 14 days [D] while MCC values were significantly higher after moderate injury compared to mild injury at low density levels only at 7 days [F] (horizontal dashed line = $P < 0.05$, 2 tailed t-test). Symbol values are group means and shaded area is standard error. Dotted line data represent pre-injury mean values of all rats for comparison.

Although we did not find a significant correlation to injury severity with any of the global variables ($P > 0.05$, data not shown), given the robust regional group differences observed in the prior data (Figs. 3–7), we investigated whether the regional values of several network parameters (strength, CC and local efficiency-EREG) were correlated to injury severity in order to evaluate the predictive potential of network-based values in acute brain injury. We found significant positive correlations among all three of the parameters at a number of brain nodes that were clustered mostly within cortical regions at 7 days, with a greater number located in the contralateral hemisphere at 7 days (22 significant positive correlations among all three network parameters obtained over 12 contralateral nodes, versus 8 correlations over 5 ipsilateral nodes, uncorrected, Fig. 10). This implies that greater derangement of network topology occurs within the side opposite to injury in rats that are more severely injured. By 14 days post-injury there were many more nodes that showed positive correlations to injury severity among the network parameters assessed (57 significant correlations from all measures over 38 nodes at 14 days compared to 20 correlations over 17 nodes at 7 days, uncorrected, Fig. 10) and although the nodal locations were bilateral in both cortical and subcortical regions, similar to 7 days there were a greater number of correlations within contralateral cortical nodes (36 correlations over 21 contralateral nodes versus 21 correlations over 17 ipsilateral nodes). By 28 days post-injury however, there were only sparse numbers of nodal correlations and unlike at the earlier time-points, this occurred among mainly ipsilateral cortical and subcortical nodes (10 significant correlations among 7 nodes, uncorrected, Fig. 10, $P < 0.05$).

At 7 days, nodal strength and EREG were the predominant parameters that positively correlated with injury severity (accounting for 45% and 42% respectively, of all correlations among the three network parameters) while at 14 days, the time-point with the greatest number of nodal correlations, CC was the predominant regional correlate (39% of all correlations), followed by nodal strength and EREG (30 and 32%, respectively). Interestingly, despite the greater clustering of strength and EREG vs severity correlations within contralateral nodes at 14 days, nodal CC vs injury severity correlations occurred in nodes equally across the brain (11 nodes per hemisphere), consistent with the measured widespread increase in CC at this time (Fig. 8B). By 28 days when far fewer nodes were correlated to injury severity, the majority of correlations occurred with ipsilateral nodal strength.

4. Discussion

4.1. Decreases in brain connectivity

The physiologic and anatomic changes underlying functional and structural changes in neuronal plasticity after brain trauma have not

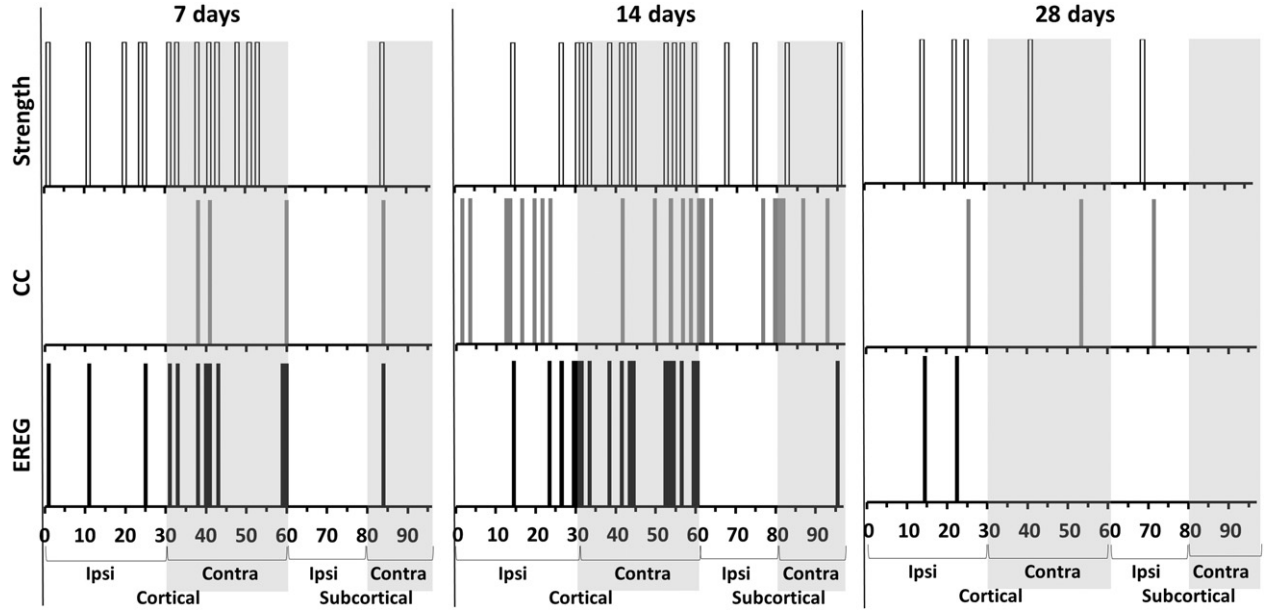

Fig. 10. Earlier but not later post-injury increases in regional network parameters of functional connectivity are associated with the degree of injury. Linear regression analysis was performed on the network parameter data (strength, local clustering coefficient [CC] and local regional efficiency [EREG]) from each of the 96 nodes for each time point after injury versus final contusion volume at 28 days. Analysis yielded significant positive correlations for all three network parameters in a number of brain regions ($P < 0.05$, r range = 0.26–0.59). Data are plotted as the presence or absence of significant nodal correlations along Y and at each brain (node) region along X at 7, 14 and 28 days post-injury. Data indicate that post-injury changes in these network parameters are associated with a change in injury severity (contusion volume) at 7 and 14 days, and this is most notable within the contralateral regions for strength and EREG at 7 and 14 days post-injury.

been extensively studied when compared to other CNS diseases such as stroke. More often than not TBI involves far more widespread disruption of brain function compared to most stroke cases on account of the white matter injury that is more prevalent after TBI. The controlled cortical impact model of TBI is a well-known model of clinical TBI that involves a contusion with significant axonal disruption when shown by diffusion tensor or kurtosis imaging (Mac Donald et al., 2007; Harris et al., 2009a; Zhuo et al., 2012) or by silver staining of sections (Hall et al., 2008). In agreement with our initial hypothesis, the deficits in interhemispheric and subcortical functional connectivity that we have shown in the present work are thus entirely expected, and generally consistent with the known structural alterations in transcallosal and cortical–thalamic disruptions after CCI injury (Mac Donald et al., 2007; Harris et al., 2009b) and in other rodent models of TBI (Donovan et al., 2014; Stemper et al., 2014; Holschneider et al., 2013). Similarly, the pericontusional deficits in functional connectivity within the ipsilateral sensorimotor regions are also congruent with both the significant alterations in fore- and hind-limb cortical somatotopic map organization (Harris et al., 2013a,b) as well as limb reaching deficits in this model (Harris et al., 2010a). Current research on whether structure and function are necessarily linked in the naïve brain is controversial and ultimately may depend on the model used for correlation (Abdelnour et al., 2014), the methodology used for analysis, or the presence or absence of CNS disease. Although the gradual, spontaneous behavioral recovery that occurs in the CCI model of brain injury does somewhat coincide with axonal reorganization (Harris et al., 2010a, b), it is notable that reductions in functional connectivity within the current study generally either persist over the same time-course as known axonal sprouting changes, or become even more deficient indicating subsequent functional disconnection and suggesting that no simple structural-functional relationship exists in this model. However, one particular regional exception was the ipsilateral M2 area of brain that temporarily increased in nodal strength rank bilaterally within the brain after injury. This is an area that consistently survives within the pericontused region in this model and which is a site for significant spontaneous sprouting after injury (Harris et al., 2010b). The likelihood of a close structural-function relationship, at least within this region is further supported by data in the same model showing that when axonal sprouting is enhanced through manipulation of the extracellular environment after injury, newly spouting axons are functionally active within the previously injured forelimb circuit (Harris et al., 2013a,b).

4.2. The injured brain is connectively promiscuous early after injury – circuit reorganization?

Although in general a structural-functional link appears either missing or regional at best after TBI, at least in regard to deficient connectivity, the relationship may be rather more complicated and involve the expansion and subsequent contraction of functional connectivity as we observed with time post-injury. The data showed that initially the injured brain becomes more connectively promiscuous after injury, with major increases in functional connectivity at 7 days that is more random, as indicated by tentative decreases found in small worldness, similar to clinical data (Nakamura et al., 2009; Pandit et al., 2013). Transient decreases in the brain's modular arrangement of its circuitry coincided temporally with this and may reflect a blurring of the boundaries between functionally connected networked compartments, possibly indicating a phase of functional reorganization. Alterations in network module connectivity have also been reported in victims of concussive blast injury, although the interpretation of this data is difficult due to the time-related changes in controls and the different imaging sites used (Han et al., 2014). While there is evidence of structural, axonal reorganization in the rat model used herein that is maximal at 7 days post-injury, with persistent low levels of sprouting to 21 days that grossly parallel the time-course of the current functional findings (Harris et al., 2010b), the biophysical mechanisms that underpin changes in functional connectivity remain to be determined and axonal sprouting may well not be the primary, or only determinant. Significant reductions in dendritic density (Jones et al., 2012) as well as spine formation occur after CCI injury in the rodent (Winston et al., 2013) that may also underlie reductions in functional connectivity through changes in receptive field size. The latter phenomenon is also suggested to occur not via structural changes but through an imbalance in excitation-inhibition (Merzenich et al., 1984; Benali et al., 2008; Mix et al., 2010;

Ding et al., 2011). Since there is good evidence for the existence of this after trauma, as indicated by reductions in GABA receptors and increased glutamate signaling (Lee et al., 2011; Raible et al., 2012; Cantu et al., 2014; Drexel et al., 2015), as well as structural alterations in the perineuronal nets on GABAergic neurons (Celio et al., 1998; Harris et al., 2009a), then changes in receptive field size and ensuing unmasking of existing or construction of new synapses, or simply changes in synaptic strength and efficacy might well underpin alterations in the observed functional connectivity. Although there is much to learn about the biology that underlies connectivity changes, it is tempting to consider whether these early network changes reflect a period of brain reorganization and whether rehabilitative "behavioral shaping" interventions would be optimally applied during or before this time to guide construction of new or repair of existing circuits. The observation of greater, albeit non-significant decreases in modularity within the mild versus moderately injured brain described here, would suggest a model by which the injury-initiated, temporary combining of circuit modules reflects a greater potential for reorganization and gain-of-function. Clearly, more experiments are required in order to empirically determine the physiologic underpinnings of functional connectivity changes post-TBI, and whether the adaptive plasticity that ensues following the loss of input to and from the brain can be faithfully modeled using rsfMRI.

4.3. Local hyper-connectedness

Despite the somewhat anticipated reductions in functional connectivity within inter-hemispheric and cortico-thalamic circuitry, the greatest surprise within the current data was the comparatively marked, widespread and persistent increases in connectivity as reflected in regional strength and clustering coefficient (CC) that were also evident globally as a reduction in characteristic shortest path (CPL) and increased in global and local efficiency (EGLOB, MELOC, respectively) within weaker connections. There is, however, precedence for this within recent clinical studies showing regional hyper-connectivity among disrupted, disconnected networks even after quite different levels of injury severity (Mayer et al., 2011; Stevens et al., 2012; Hillary et al., 2014). Similar increases in EGLOB and MELOC, reductions in CPL have been shown clinically at 3 months after moderate TBI (Nakamura et al., 2009). The hyper-connectivity appears to be a transient event after experimental TBI since the levels attained at 7 days did not persist, although they remained evident within bilateral S2 and some S1 cortical regions, as well as in ipsi-lesional thalamus and caudate, and bilaterally in the hippocampus at 4 weeks post-injury, possibly indicating some residual potential for reorganization in these regions. While this initial "functional pruning" might be a physiologic response indicative of reorganization, hyper-connectivity itself is likely to be metabolically costly so that alternative-fuel-based neuroprotective interventions after TBI (Fukushima et al., 2009) might well extend this period and allow for more chronic rehabilitative interventions. Given the highly compressed time-scale of recovery in the brain-injured rodent compared to human, it remains plausible that future longitudinal studies might discover that the period of hyper-connectivity could be a biomarker of the most efficacious time post-injury to begin rehabilitative interventions.

The hyper-connectivity appears to have a complex temporal component, with increased random connectivity indicated by reduced normalized CPL that is limited to acute time points, but followed chronically by persistent decreases in CPL and increases in CC and MELOC. This acute-to-chronic shift towards more local connectivity with increased efficiency indicates better network performance, with the potential for information transfer to be maintained over longer distances. However, it must be acknowledged that reductions in average CPL might also, or alternatively occur due to the significant structural disturbance that conceivably might have a greater effect on longer rather than shorter paths. This would then suggest that reduced CPL occurs merely due to the weighted average towards short paths - a less likely phenomenon given the spontaneous functional recovery that occurs in this model. Therefore in support of the former theory that reduced CPL indicates enhanced local connectivity after injury, increased neuronal correlated activity in the monkey was found to be limited only to regions undergoing reorganization following induction of cortical map plasticity (Dinse et al., 1993). Similar correlated activity changes, albeit at the level of BOLD and not direct neuronal activity was seen in the current data within pericontusional and homotopic cortex, regions that have been shown to undergo significant changes in map plasticity (Harris et al., 2013a,b). These data would therefore concur with a hypothesis that TBI results in increased level of local connectedness primarily within regions undergoing reorganization as a compensatory measure to offset the loss in functional homeostasis.

In terms of network architecture, these hyperconnectivity data would support a model of Hebbian type plasticity (Hebb, 1949) through one of the aforementioned physiologic mechanisms whereby synaptic strengthening occurs via co-activated inputs leading to enhanced local connectivity. The tentative finding of an early, temporary loss of the small world network property would reflect a temporary scale free network asserting itself (de Arcangelis and Herrmann, 2012) prior to prevailing homeostatic mechanisms resetting global network excitability to promote functional pruning in order to reestablish more normal or even novel network patterns. On the other hand however, it is also worth considering that the observed decreased path length implies the connections become more random since low path and the observed high clustering is a defining characteristic of a random network. It remains to be seen whether this reflects the development of aberrant plasticity or whether this is simply an initial stage of functional reorganization. Finally, it is conceivable that different mechanisms of functional recovery drive different connectivity parameters. For example, the spatial distribution of nodes with increased CC was far more widespread than nodes with increased strength, and this could indicate wider cortical recruitment versus more focal consolidation of function.

The most highly connected hubs in the rat brain — caudate, thalamus, M1 and barrel field cortex remained dominant in their connectivity in the brain even after injury, and this is in agreement with clinical data showing that the change in connectivity is disproportionally represented in regions belonging to the brain's core networks (Hillary et al., 2014). This may indicate some degree of network resilience to the effects of injury in that the most highly connected hubs act to buffer the level of network disruption. This is supported by the fact that there were no decreases in EGLOB among the stronger connections (1–20% network density) even despite there being a global reduction in CPL among all levels of connectivity.

4.4. Injury severity-importance of the contralateral cortex

Global network measures did not correlate with injury severity possibly indicating that either the measures were not sensitive to the increasing severity of injury, or that compensatory functional adaption of the remaining parenchyma occurred. However, considering the robust trends in the global data grouped by severity level (Fig. 9), it would seem just as likely that the number of data points were too low to achieve significance. The observation that early, transient reductions in modularity was greater among mildly injured than moderately injured brains is interesting because the reduction in CPL and increase in mean CC were greatest among moderately injured brains. This would suggest that either different physiologic mechanism drive these parameters or possibly that changes in modularity are a more sensitive indicator of reorganization.

The regional correlations of EREG, CC and strength indicate that injury severity-linked increases in these parameters occurs in locally discrete regions for strength and efficiency, with the contralateral cortex being the site of most significant change in relation to the degree of injury. Once again this is not an unexpected finding given the contralateral shift in the affected forelimb cortical map that occurs after injury in this model (Harris et al., 2003). Within the confines of the current

data this effect was maximal at 14 days and this temporally corresponds to the development of contralateral hyper-excitability in this model (Verley et al., 2013). While both of these effects may be related to overuse of the unaffected limb, injury to the corpus callosum has been shown to have significant effects on the correlated BOLD signal (Magnuson et al., 2014a) so that contralateral changes may well reflect CNS level rather than, or in addition to, activity-dependent circuit changes. The relative absence of significant network parameter correlations at 28 days post-injury suggests that the brain has functionally compensated for the loss of homeostasis and this would be consistent with the relatively complete spontaneous recovery of function in this injury model, at this time post-injury. The brain-wide phenomenon of increasing CC with injury severity that is generally only prominent at 14 days post-injury in these data indicate the reliance of the more severely injured brains on local connectivity. However, it remains to be seen whether the timing of these changes points to the existence of a temporal watershed beyond which reorganization is less malleable.

4.5. Study limitations

After TBI in particular, there is a need to be cautious over the interpretation of the correlations in basal blood-oxygen-level-dependent (BOLD) signal with regard to the upstream neuronal activity, on account of any disease-related conditions that might alter the neurovascular coupling, the whole basis for the BOLD signal (Mayer et al., 2014; Mishra et al., 2011). While there are significant decreases in blood flow (Richards et al., 1995; Chen et al., 2004) and electrophysiologic activity (Shaw and Cant, 1984) acutely after CCI injury, blood-flow elicited response to forelimb stimulation suggest that coupling may be intact by 4 days post-injury (Harris et al., 2013a,b), preventing any confound in the data at 7 days. Regardless, the majority of the connectivity changes were not solely focused on the ipsilateral cortex, the region most likely to be affected by uncoupling so that any confound due to uncoupling is likely to be minimized at the post-injury times studied in this work. Early decreases in intrinsic T2* (decay of transverse magnetization in a gradient-echo image mainly due to magnetic field inhomogeneity) occur in this model due to hemorrhage-related products within the brain parenchyma, and this will also confound data interpretation within the ipsilateral, pericontused region. While this will most certainly result in spurious connectivity changes acutely, including increased connectivity within the pericontused hemorrhagic regions and decreased to other brain regions, the majority of the changes were wide-spread increased connectivity that could not be accounted for by local hemorrhagic changes in T2*. It should be noted that connectivity changes obtained in this study are based on correlative analysis, and that future use of effective connectivity measures modeled through techniques such as structural equation modeling, dynamic causal modeling or granger causality, ideally in conjunction with optogenetic-based brain silencing measures or direct electrophysiologic data, is required to fully understand injury-related changes in connectivity. Finally, the TBI model used here represents only some aspects of clinical TBI pathology and does not capture the often more widespread axonal damage that occurs in non-penetrating impact acceleration models in larger animals such as swine or primates.

To conclude, we have shown that the post-injury TBI period is characterized by significant changes in global network parameters resulting in a reliance on more local functional connectivity especially after more severe injury. While regional reductions in connectivity were largely predicted based on prior structural and physiologic data, hyperconnectivity was an unexpected finding that was prevalent in regions known to undergo reorganization. Given that these findings have already been demonstrated clinically, future longitudinal studies are warranted to examine both the biophysical underpinnings of this and also the potential use of these network parameters as a marker for functional plasticity.

Funding source

UCLA Brain Injury Research Center; NIH NINDS NS091222; NS27544; NGH is a fellow of the Center for Neuroskills, Bakersfield, California.

References

Abdelnour, F., Voss, H.U., Raj, A., 2014. Network diffusion accurately models the relationship between structural and functional brain connectivity networks. NeuroImage 90, 335–347. http://dx.doi.org/10.1016/j.neuroimage.2013.12.039.

de Arcangelis, L., Herrmann, H.J., 2012. Activity-dependent neuronal model on complex networks. Front. Physiol. 3, 1–9. http://dx.doi.org/10.3389/fphys.2012.00062 (MAR).

Benali, A., Weiler, E., Benali, Y., et al., 2008. Excitation and inhibition jointly regulate cortical reorganization in adult rats. J. Neurosci. 28, 12284–12293. http://dx.doi.org/10.1523/JNEUROSCI.1952-08.2008.

Biswal, B., Yetkin, F.Z., Haughton, V.M., Hyde, J.S., 1995. Functional connectivity in the motor cortex of resting human brain using echo-planar MRI. Magn. Reson. Med. 34, 537–541.

Blondel, V.D., Guillaume, J.-L., Lambiotte, R., Lefebvre, E., 2008. Fast unfolding of communities in large networks. J. Stat. Mech. 10, P10008. http://dx.doi.org/10.1088/1742-5468/2008/10/P10008.

Cantu, D., Walker, K., Andresen, L., et al., 2014. Traumatic brain injury increases cortical glutamate network activity by compromising GABAergic control. Cereb. Cortex http://dx.doi.org/10.1093/cercor/bhu041.

Celio, M.R., Spreafico, R., De Biasi, S., Vitellaro-Zuccarello, L., 1998. Perineuronal nets: past and present. Trends Neurosci. 21, 510–515.

Chen, S., Pickard, J.D., Harris, N.G., 2003. Time course of cellular pathology after controlled cortical impact injury. Exp. Neurol. 182, 87–102.

Chen, S., Richards, H.K., Smielewski, P., et al., 2002. Preventing flow-metabolism uncoupling acutely reduces evolving axonal injury after traumatic brain injury. J. Neurotrauma 19, 1300.

Chen, S.F., Richards, H.K., Smielewski, P., et al., 2004. Relationship between flow-metabolism uncoupling and evolving axonal injury after experimental traumatic brain injury. J. Cereb. Blood Flow Metab. 24, 1025–1036.

Crum, W.R., Giampietro, V.P., Smith, E.J., et al., 2013. A comparison of automated anatomical–behavioural mapping methods in a rodent model of stroke. J. Neurosci. Methods 218, 170–183. http://dx.doi.org/10.1016/j.jneumeth.2013.05.009.

David, O., Guillemain, I., Saillet, S., et al., 2008. Identifying neural drivers with functional MRI: an electrophysiological validation. PLoS Biol. 6, 2683–2697. http://dx.doi.org/10.1371/journal.pbio.0060315.

Ding, M.-C., Wang, Q., Lo, E.H., Stanley, G.B., 2011. Cortical excitation and inhibition following focal traumatic brain injury. J. Neurosci. 31, 14085–14094. http://dx.doi.org/10.1523/JNEUROSCI.3572-11.2011.

Dinse, H.R., Recanzone, G.H., Merzenich, M.M., 1993. Alterations in correlated activity parallel ICMS-induced representational plasticity. Neuroreport 5, 173–176.

Donovan, V., Kim, C., Anugerah, A.K., et al., 2014. Repeated mild traumatic brain injury results in long-term white-matter disruption. J. Cereb. Blood Flow Metab. 34, 715–723. http://dx.doi.org/10.1038/jcbfm.2014.6.

Drexel, M., Puhakka, N., Kirchmair, E., et al., 2015. Expression of GABA receptor subunits in the hippocampus and thalamus after experimental traumatic brain injury. Neuropharmacology 88, 122–133. http://dx.doi.org/10.1016/j.neuropharm.2014.08.023.

Fukushima, M., Lee, S.M., Moro, N., et al., 2009. Metabolic and histologic effects of sodium pyruvate treatment in the rat after cortical contusion injury. J. Neurotrauma 26, 1095–1110. http://dx.doi.org/10.1089/neu.2008.0771.

Gennarelli, T.A., Thibault, L.E., Adams, J.H., et al., 1982. Diffuse axonal injury and traumatic coma in the primate. Ann. Neurol. 12, 564–574. http://dx.doi.org/10.1002/ana.410120611.

Graham, D.I., Adams, J.H., Nicoll, J.A., et al., 1995. The nature, distribution and causes of traumatic brain injury. Brain Pathol. 5, 397–406.

Hall, E.D., Bryant, Y.D., Cho, W., Sullivan, P.G., 2008. Evolution of post-traumatic neurodegeneration after controlled cortical impact traumatic brain injury in mice and rats as assessed by the de Olmos silver and fluorojade staining methods. J. Neurotrauma 25, 235–247. http://dx.doi.org/10.1089/neu.2007.0383.

Han, K., Mac Donald, C.L., Johnson, A.M., et al., 2014. Disrupted modular organization of resting-state cortical functional connectivity in U.S. military personnel following concussive "mild" blast-related traumatic brain injury. NeuroImage 84, 76–96. http://dx.doi.org/10.1016/j.neuroimage.2013.08.017.

Harris, N.G., Carmichael, S.T., Hovda, D.A., Sutton, R.L., 2009a. Traumatic brain injury results in disparate regions of chondroitin sulfate proteoglycan expression that are temporally limited. J. Neurosci. Res. 87, 2937–2950. http://dx.doi.org/10.1002/jnr.22115.

Harris, N.G., Chen, S.F., Pickard, J.D., 2003. Reorganisation after experimental traumatic brain injury: a functional autoradiography study. J. Cereb. Metab. Blood FLow 21, 1318.

Harris, N.G., Chen, S.-F., Pickard, J., 2013a. Cortical reorganisation after experimental traumatic brain injury: a functional autoradiography study. J. Neurotrauma http://dx.doi.org/10.1089/neu.2012.2785.

Harris, N.G., Hovda, D.A., Sutton, R.L., 2009b. Acute deficits in transcallosal connectivity endure chronically after experimental brain injury in the rat: a dti tractography study. J. Neurotrauma 26, A37.

Harris, N.G., Mironova, Y.A., Chen, S.-F., et al., 2012. Preventing flow-metabolism uncoupling acutely reduces axonal injury after traumatic brain injury. J. Neurotrauma 29, 1469–1482. http://dx.doi.org/10.1089/neu.2011.2161.

Harris, N.G., Mironova, Y.A., Hovda, D.A., Sutton, R.L., 2010a. Chondroitinase ABC enhances pericontusion axonal sprouting but does not confer robust improvements in behavioral recovery. J. Neurotrauma 27, 1–12. http://dx.doi.org/10.1089/neu.2010.1470.
Harris, N.G., Mironova, Y.A., Hovda, D.A., Sutton, R.L., 2010b. Pericontusion axon sprouting is spatially and temporally consistent with a growth-permissive environment after traumatic brain injury. J. Neuropathol. Exp. Neurol. 69, 139–154. http://dx.doi.org/10.1097/NEN.0b013e3181cb5bee.
Harris, N.G., Nogueira, M.S.M., Verley, D.R., Sutton, R.L., 2013b. Chondroitinase enhances cortical map plasticity and increases functionally active sprouting axons after brain injury. J. Neurotrauma 30, 1257–1269. http://dx.doi.org/10.1089/neu.2012.2737.
Hebb, D., 1949. The Organization of Behavior. Wiley & Sons, New York.
Hillary, F.G., Rajtmajer, S.M., Roman, C.A., et al., 2014. The rich get richer: brain injury elicits hyperconnectivity in core subnetworks. PLoS One 9, e104021. http://dx.doi.org/10.1371/journal.pone.0104021.
Holschneider, D.P., Guo, Y., Wang, Z., et al., 2013. Remote brain network changes after unilateral cortical impact injury and their modulation by acetylcholinesterase inhibition. J. Neurotrauma 30, 907–919. http://dx.doi.org/10.1089/neu.2012.2657.
Jenkinson, M., Smith, S., 2001. A global optimisation method for robust affine registration of brain images. Med. Image Anal. 5, 143–156.
Jenkinson, M., Bannister, P., Brady, M., Smith, S., 2002. Improved optimization for the robust and accurate linear registration and motion correction of brain images. NeuroImage 17, 825–841.
Jones, T.A., Liput, D.J., Maresh, E.L., et al., 2012. Use-dependent dendritic regrowth is limited after unilateral controlled cortical impact to the forelimb sensorimotor cortex. J. Neurotrauma 29, 1455–1468. http://dx.doi.org/10.1089/neu.2011.2207.
Kalthoff, D., Seehafer, J.U., Po, C., et al., 2011. Functional connectivity in the rat at 11.7T: impact of physiological noise in resting state fMRI. NeuroImage 54, 2828–2839. http://dx.doi.org/10.1016/j.neuroimage.2010.10.053.
Kasahara, M., Menon, D.K., Salmond, C.H., et al., 2010. Altered functional connectivity in the motor network after traumatic brain injury. Neurology 75, 168–176. http://dx.doi.org/10.1212/WNL.0b013e3181e7ca58.
Kasahara, M., Menon, D.K., Salmond, C.H., et al., 2011. Traumatic brain injury alters the functional brain network mediating working memory. Brain Inj. 25, 1170–1187. http://dx.doi.org/10.3109/02699052.2011.608210.
Lee, S., Ueno, M., Yamashita, T., 2011. Axonal remodeling for motor recovery after traumatic brain injury requires downregulation of γ-aminobutyric acid signaling. Cell Death Dis. 2, e133. http://dx.doi.org/10.1038/cddis.2011.16.
Liang, Z., King, J., Zhang, N., 2012. Intrinsic organization of the anesthetized brain. J. Neurosci. 32, 10183–10191.
Mac Donald, C.L., Dikranian, K., Song, S.K., et al., 2007. Detection of traumatic axonal injury with diffusion tensor imaging in a mouse model of traumatic brain injury. Exp. Neurol. 205, 116–131. http://dx.doi.org/10.1016/j.expneurol.2007.01.035.
Magnuson, M.E., Thompson, G.J., Pan, W.-J., Keilholz, S.D., 2014a. Effects of severing the corpus callosum on electrical and BOLD functional connectivity and spontaneous dynamic activity in the rat brain. Brain Connect. 4, 15–29. http://dx.doi.org/10.1089/brain.2013.0167.
Magnuson, M.E., Thompson, G.J., Pan, W.-J., Keilholz, S.D., 2014b. Time-dependent effects of isoflurane and dexmedetomidine on functional connectivity, spectral characteristics, and spatial distribution of spontaneous BOLD fluctuations. NMR Biomed. 27, 291–303. http://dx.doi.org/10.1002/nbm.3062.
Mayer, A.R., Mannell, M.V., Ling, J., et al., 2011. Functional connectivity in mild traumatic brain injury. Hum. Brain Mapp. 32, 1825–1835. http://dx.doi.org/10.1002/hbm.21151.
Mayer, A.R., Toulouse, T., Klimaj, S., et al., 2014. Investigating the properties of the hemodynamic response function after mild traumatic brain injury. J. Neurotrauma 31 (2), 189–197. http://dx.doi.org/10.1089/neu.2013.3069.
Merzenich, M.M., Nelson, R.J., Stryker, M.P., et al., 1984. Somatosensory cortical map changes following digit amputation in adult monkeys. J. Comp. Neurol. 224, 591–605. http://dx.doi.org/10.1002/cne.902240408.
Mishra, A.M., Bai, X., Sanganahalli, B.G., et al., 2014. Decreased resting functional connectivity after traumatic brain injury in the rat. PLoS One 9, e95280. http://dx.doi.org/10.1371/journal.pone.0095280.
Mishra, A.M., Ellens, D.J., Schridde, U., et al., 2011. Where fMRI and electrophysiology agree to disagree: corticothalamic and striatal activity patterns in the WAG/Rij rat. J. Neurosci. 31 (42), 15053–15064. http://dx.doi.org/10.1523/JNEUROSCI.0101-11.2011.
Mix, A., Benali, A., Eysel, U.T., Funke, K., 2010. Continuous and intermittent transcranial magnetic theta burst stimulation modify tactile learning performance and cortical protein expression in the rat differently. Eur. J. Neurosci. 32, 1575–1586. http://dx.doi.org/10.1111/j.1460-9568.2010.07425.x.
Nakamura, T., Hillary, F.G., Biswal, B.B., 2009. Resting network plasticity following brain injury. PLoS One 4, e8220. http://dx.doi.org/10.1371/journal.pone.0008220.
Pan, W.-J., Thompson, G.J., Magnuson, M.E., et al., 2013. Infraslow LFP correlates to resting-state fMRI BOLD signals. NeuroImage 74, 288–297. http://dx.doi.org/10.1016/j.neuroimage.2013.02.035.
Pandit, A.S., Expert, P., Lambiotte, R., et al., 2013. Traumatic brain injury impairs small-world topology. Neurology 80, 1826–1833. http://dx.doi.org/10.1212/WNL.0b013e3182929f38.
Paxinos, G., Watson, C., 1997. The Rat Brain in Stereotaxic Coordinates. Academic Press, New York.
Raible, D.J., Frey, L.C., Cruz Del Angel, Y., et al., 2012. GABA(a) receptor regulation after experimental traumatic brain injury. J. Neurotrauma 29, 2548–2554. http://dx.doi.org/10.1089/neu.2012.2483.
Rehme, A.K., Eickhoff, S.B., Wang, L.E., et al., 2011. Dynamic causal modeling of cortical activity from the acute to the chronic stage after stroke. NeuroImage 55, 1147–1158. http://dx.doi.org/10.1016/j.neuroimage.2011.01.014.
Reyt, S., Picq, C., Sinniger, V., et al., 2010. Dynamic causal modelling and physiological confounds: a functional MRI study of vagus nerve stimulation. NeuroImage 52, 1456–1464. http://dx.doi.org/10.1016/j.neuroimage.2010.05.021.
Richards, H.K., Bucknall, R.M., Jones, H.C., Pickard, J.D., 1995. Uncoupling of LCBF and LCGU in two different models of hydrocephalus: a review. Childs Nerv. Syst. 11, 288–292.
Rubinov, M., Sporns, O., 2010. Complex network measures of brain connectivity: uses and interpretations. NeuroImage 52, 1059–1069.
Shattuck, D.W., Leahy, R.M., 2002. BrainSuite: an automated cortical surface identification tool. Med. Image Anal. 6, 129–142.
Shaw, N.A., Cant, B.R., 1984. The effect of experimental concussion on somatosensory evoked potentials. Aust. J. Exp. Biol. Med. Sci. 62 (Pt 3), 361–371.
Smith, S.M., 2002. Fast robust automated brain extraction. Hum. Brain Mapp. 17, 143–155. http://dx.doi.org/10.1002/hbm.10062.
Smith, S.M., Jenkinson, M., Woolrich, M.W., et al., 2004. Advances in functional and structural MR image analysis and implementation as FSL. NeuroImage 23 (Suppl. 1), S208–S219. http://dx.doi.org/10.1016/j.neuroimage.2004.07.051.
Stemper, B.D., Shah, A.S., Pintar, F.a., et al., 2014. Head rotational acceleration characteristics influence behavioral and diffusion tensor imaging outcomes following concussion. Ann. Biomed. Eng. http://dx.doi.org/10.1007/s10439-014-1171-9.
Stevens, M.C., Lovejoy, D., Kim, J., et al., 2012. Multiple resting state network functional connectivity abnormalities in mild traumatic brain injury. Brain Imaging Behav. 6, 293–318. http://dx.doi.org/10.1007/s11682-012-9157-4.
Valdés-Hernández, P.A., Sumiyoshi, A., Nonaka, H., et al., 2011. An in vivo MRI template set for morphometry, tissue segmentation, and fMRI localization in rats. Front. Neuroinform. 5, 26. http://dx.doi.org/10.3389/fninf.2011.00026.
van Meer, M.P.A., van der Marel, K., Wang, K., et al., 2010. Recovery of sensorimotor function after experimental stroke correlates with restoration of resting-state interhemispheric functional connectivity. J. Neurosci. 30, 3964–3972. http://dx.doi.org/10.1523/JNEUROSCI.5709-09.2010.
Verley, D.R., Gutman, B.A., Harris, N.G., 2013. Delayed increases in contra-contusional hyper-excitability underlie trans-hemispheric cortical activation following traumatic brain injury: evidence of contra-contusional involvement in recovery of limb function. J. Neurotrauma 30, a121.
Wang, L., Yu, C., Chen, H., et al., 2010. Dynamic functional reorganization of the motor execution network after stroke. Brain 133, 1224–1238. http://dx.doi.org/10.1093/brain/awq043.
Williams, K.A., Magnuson, M., Majeed, W., et al., 2010. Comparison of alpha-chloralose, medetomidine and isoflurane anesthesia for functional connectivity mapping in the rat. Magn. Reson. Imaging 28, 995–1003. http://dx.doi.org/10.1016/j.mri.2010.03.007.
Winston, C.N., Chellappa, D., Wilkins, T., et al., 2013. Controlled cortical impact results in an extensive loss of dendritic spines that is not mediated by injury-induced amyloid-beta accumulation. J. Neurotrauma 30, 1966–1972. http://dx.doi.org/10.1089/neu.2013.2960.
Xia, M., Wang, J., He, Y., 2013. BrainNet viewer: a network visualization tool for human brain connectomics. PLoS One 8, e68910. http://dx.doi.org/10.1371/journal.pone.0068910.
Yushkevich, P.A., Piven, J., Hazlett, H.C., et al., 2006. User-guided 3D active contour segmentation of anatomical structures: significantly improved efficiency and reliability. NeuroImage 31, 1116–1128. http://dx.doi.org/10.1016/j.neuroimage.2006.01.015.
Zhou, Y., Lui, Y.W., Zuo, X.-N., et al., 2013. Characterization of thalamo-cortical association using amplitude and connectivity of functional MRI in mild traumatic brain injury. J. Magn. Reson. Imaging http://dx.doi.org/10.1002/jmri.24310.
Zhuo, J., Xu, S., Proctor, J.L., et al., 2012. Diffusion kurtosis as an in vivo imaging marker for reactive astrogliosis in traumatic brain injury. NeuroImage 59, 467–477. http://dx.doi.org/10.1016/j.neuroimage.2011.07.050.